Substitution of a single non-coding nucleotide upstream of *TMEM216* causes non-syndromic retinitis pigmentosa and is associated with reduced *TMEM216* expression

Graphical abstract

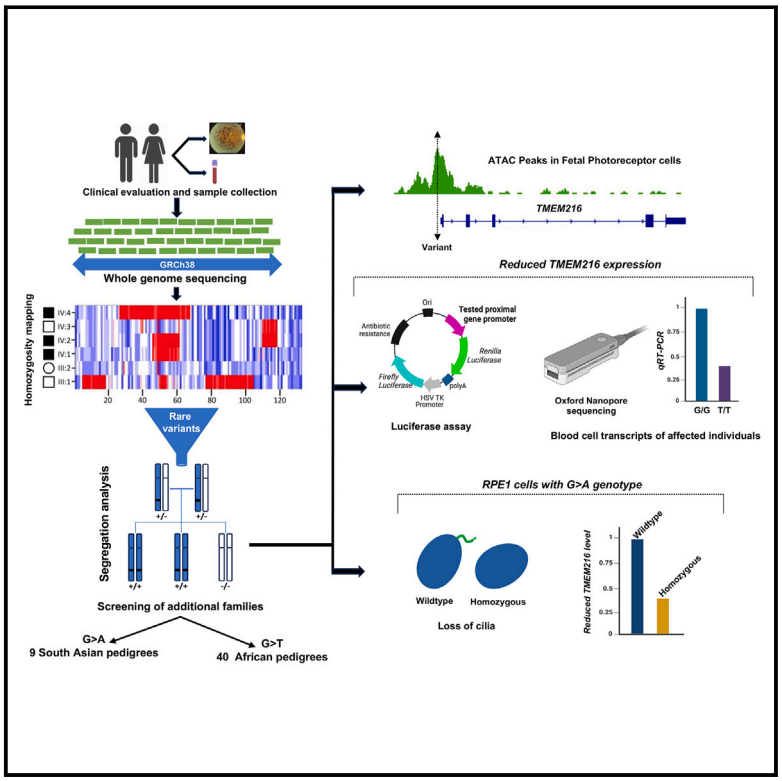

Authors

Samantha Malka, Pooja Biswas, Anne-Marie Berry, ..., Gavin Arno, Andrew R. Webster, Radha Ayyagari

Correspondence

andrew.webster@ucl.ac.uk (A.R.W.), rayyagari@health.ucsd.edu (R.A.)

Genetic analyses of retinitis pigmentosa (RP)-affected individuals in African and Pakistani populations, along with functional validations, identified two novel pathogenic substitutions in the UTR of *TMEM216*: c.−69G>T and c.−69G>A. The c.−69G>T variant is estimated to account for about 20% of RP cases in individuals of African ancestry, including African Americans.

Malka et al., 2024, The American Journal of Human Genetics *111*, 2012–2030
September 5, 2024 © 2024 The Authors.
https://doi.org/10.1016/j.ajhg.2024.07.020

ARTICLE

Substitution of a single non-coding nucleotide upstream of *TMEM216* causes non-syndromic retinitis pigmentosa and is associated with reduced *TMEM216* expression

Samantha Malka,[1,2,32] Pooja Biswas,[3,32] Anne-Marie Berry,[3,32] Riccardo Sangermano,[4] Mukhtar Ullah,[5,6] Siying Lin,[1,2] Matteo D'Antonio,[7] Aleksandr Jestin,[2] Xiaodong Jiao,[8] Mathieu Quinodoz,[5,6,9] Lori Sullivan,[10] Jessica C. Gardner,[2] Emily M. Place,[4] Michel Michaelides,[1,2] Karolina Kaminska,[5,6] Omar A. Mahroo,[1,2,11,12] Elena Schiff,[1,2] Genevieve Wright,[1,2] Francesca Cancellieri,[5,6] Veronika Vaclavik,[13] Cristina Santos,[15,16] Atta Ur Rehman,[17] Sudeep Mehrotra,[4] Hafiz Muhammad Azhar Baig,[4] Muhammad Iqbal,[18] Muhammad Ansar,[13,14] Luisa Coutinho Santos,[15] Ana Berta Sousa,[19,20] Viet H. Tran,[13,31] Hiroko Matsui,[3] Anjana Bhatia,[3] Muhammad Asif Naeem,[21] Shehla J. Akram,[22] Javed Akram,[23,24] Sheikh Riazuddin,[24,25] Carmen Ayuso,[25,26] Eric A. Pierce,[4] Alison J. Hardcastle,[2] S. Amer Riazuddin,[27] Kelly A. Frazer,[28,29] J. Fielding Hejtmancik,[8] Carlo Rivolta,[5,6,9,33] Kinga M. Bujakowska,[4,33] Gavin Arno,[1,2,30,33] Andrew R. Webster,[1,2,33,*] and Radha Ayyagari[3,33,*]

Summary

Genome analysis of individuals affected by retinitis pigmentosa (RP) identified two rare nucleotide substitutions at the same genomic location on chromosome 11 (g.61392563 [GRCh38]), 69 base pairs upstream of the start codon of the ciliopathy gene *TMEM216* (c.−69G>A, c.−69G>T [GenBank: NM_001173991.3]), in individuals of South Asian and African ancestry, respectively. Genotypes included 71 homozygotes and 3 mixed heterozygotes in *trans* with a predicted loss-of-function allele. Haplotype analysis showed single-nucleotide variants (SNVs) common across families, suggesting ancestral alleles within the two distinct ethnic populations. Clinical phenotype analysis of 62 available individuals from 49 families indicated a similar clinical presentation with night blindness in the first decade and progressive peripheral field loss thereafter. No evident systemic ciliopathy features were noted. Functional characterization of these variants by luciferase reporter gene assay showed reduced promotor activity. Nanopore sequencing confirmed the lower transcription of the *TMEM216* c.−69G>T allele in blood-derived RNA from a heterozygous carrier, and reduced expression was further recapitulated by qPCR, using both leukocytes-derived RNA of c.−69G>T homozygotes and total RNA from genome-edited hTERT-RPE1 cells carrying homozygous *TMEM216* c.−69G>A. In conclusion, these variants explain a significant proportion of unsolved cases, specifically in individuals of African ancestry, suggesting that reduced *TMEM216* expression might lead to abnormal ciliogenesis and photoreceptor degeneration.

Introduction

Retinitis pigmentosa (RP [MIM: 613731]), the largest clinical subset of inherited retinal disorders (IRDs), is characterized by progressive degeneration of rod photoreceptor cells. RP is estimated to affect approximately 1 in 2,500 to 4,000 individuals worldwide, typically presenting with night blindness, followed by the gradual constriction of the visual field,

[1]Moorfields Eye Hospital NHS Trust, London, UK; [2]UCL Institute of Ophthalmology, University College London, London, UK; [3]Shiley Eye Institute, University of California, San Diego, San Diego, CA, USA; [4]Ocular Genomics Institute, Massachusetts Eye and Ear Infirmary, Department of Ophthalmology, Harvard Medical School, Boston, MA, USA; [5]Institute of Molecular and Clinical Ophthalmology Basel (IOB), Basel, Switzerland; [6]Department of Ophthalmology, University of Basel, Basel, Switzerland; [7]Department of Medicine, Division of Biomedical Informatics, University of California, San Diego, La Jolla, CA, USA; [8]Ophthalmic Genetics and Visual Function Branch, National Eye Institute, National Institutes of Health, Bethesda, MD 20892, USA; [9]Department of Genetics and Genome Biology, University of Leicester, Leicester, UK; [10]Human Genetics Center, School of Public Health, University of Texas Health Science Center, Houston, TX, USA; [11]Department of Ophthalmology, St Thomas' Hospital, London, UK; [12]Section of Ophthalmology, King's College London, St Thomas' Hospital Campus, London, UK; [13]Hôpital Ophtalmique Jules-Gonin, Lausanne, Switzerland; [14]Advanced Molecular Genetics and Genomics Disease Research and Treatment Centre, Dow University of Health Sciences, Karachi 74200, Pakistan; [15]Instituto de Oftalmologia Dr. Gama Pinto (IOGP), Lisboa, Portugal; [16]Faculdade de Ciências Médicas, NMS, FCM, NOVA Medical School, Universidade NOVA de Lisboa, 7 iNOVA4Health, Lisboa, Portugal; [17]Department of Zoology, Faculty of Biological and Health Sciences, Hazara University, Mansehra 21300, Khyber Pakhtunkhwa, Pakistan; [18]Department of Biotechnology, Institute of Biochemistry, Biotechnology and Bioinformatics, The Islamia University of Bahawalpur, Bahawalpur 63100, Pakistan; [19]Medical Genetics Unit, Hospital Pediátrico, Centro Hospitalar e Universitário de Lisboa Norte (CHULN), Lisboa, Portugal; [20]Serviço de Genética Médica, Departamento de Pediatria, Hospital de Santa Maria, Lisboa, Portugal; [21]National Centre of Excellence in Molecular Biology, University of the Punjab, Lahore, Pakistan; [22]Akram Medical Complex, Lahore, Pakistan; [23]Allama Iqbal Medical Research Center, Lahore, Pakistan; [24]Jinnah Burn and Reconstructive Surgery Center, Jinnah Hospital, Lahore, Pakistan; [25]Department of Genetics, Health Research Institute-Fundación Jiménez Díaz University Hospital, Universidad Autónoma de Madrid (IIS-FJD, UAM), 28049 Madrid, Spain; [26]Center for Biomedical Network Research on Rare Diseases (CIBERER), Instituto de Salud Carlos III, Madrid, Spain; [27]The Wilmer Eye Institute, Johns Hopkins University School of Medicine, Baltimore, MD, USA; [28]Department of Pediatrics, University of California, San Diego, La Jolla, CA, USA; [29]Institute of Genomic Medicine, University of California, San Diego, La Jolla, CA, USA; [30]Greenwood Genetic Center, Greenwood, SC, USA; [31]Centre for Gene Therapy and Regenerative Medicine, King's College London, London, UK
[32]These authors contributed equally
[33]These authors contributed equally
*Correspondence: andrew.webster@ucl.ac.uk (A.R.W.), rayyagari@health.ucsd.edu (R.A.)
https://doi.org/10.1016/j.ajhg.2024.07.020.
© 2024 The Authors. This is an open access article under the CC BY-NC-ND license (http://creativecommons.org/licenses/by-nc-nd/4.0/).

often leading to legal blindness.[1–3] Fundus abnormalities include bone spicule-like pigment deposits in the peripheral retina, attenuation of retinal vessels, and a pale optic nerve head. For individuals who undergo genetic testing, there is a significantly lower rate of molecular diagnosis in ethnicities that are under-represented in aggregated genome datasets.[1,4,5] Missing molecular diagnoses may be attributed to non-coding variants, structural rearrangements, variants in unreported RP genes, and incorrect clinical diagnosis.[1,4,6–8]

Pathogenic variants in over 280 IRD genes have been identified across all Mendelian inheritance patterns (RetNet database, https://sph.uth.edu/RetNet/). Variants impacting protein-coding genes involved in various pathways including phototransduction, photoreceptor structure, ciliogenesis, and RNA splicing have been identified as causes of syndromic and non-syndromic IRDs.[7,9–11] Many IRDs are classified as ciliopathies, with variants in genes that are involved with cilia biogenesis and transport.[12–17] Variants in ciliary genes can cause a spectrum of phenotypes ranging from non-syndromic retinal degenerations to syndromic ciliopathies.[18–23]

This study identified two candidate pathogenic variants on chromosome 11 at the genomic position g.61392563 (GRCh38) upstream of *TMEM216* (c.−69G>T, c.−69G>A, GenBank: NM_001173991.3; MIM: 613277) and 23 kb downstream of *TMEM138* (MIM: 614459). These variants were identified in a total of 74 individuals affected with RP of African (c.−69G>T) and South Asian (c.−69G>A) ancestry. Variants in both *TMEM216* and *TMEM138* have previously been implicated in Joubert (MIM: 608091) and Meckel (MIM: 603194) syndromes, often exhibiting retinal findings.[24–26] The expression of these genes is regulated by the conserved regulatory elements located in the intergenic region.[25] Variants in *TMEM216* and *TMEM138* identified to date in Joubert or Meckel syndrome are limited to the coding region and splice sites with a likely loss, or reduced, function as the disease mechanism.[24,27–29]

Subjects and methods

Ethical statement

All studies were performed in accordance with the Declaration of Helsinki and the approval of the institutional review boards (IRB) of University of California San Diego, La Jolla, CA, USA; Johns Hopkins University, Baltimore, MD, USA; the CNS IRB at the National Institutes of Health, Bethesda, MD, USA; Moorfields Eye Hospital, London UK (Genetic Study of Inherited Eye Disease Research Ethics Committee [REC] ref. 12/LO/0141) or Genomics England 100,000 Genomes project (REC ref. 14/EE/1112) or NIHR BioResource for Rare Disease (REC ref. 13/EE/0325); the Ethikkommission Nordwest-und Zentralschweiz; the Commission Cantonale d'Étique de la Recherche sur l'Être Humain du Canton de Vaud; the Comissão de Ética para a Saúde do Instituto de Oftalmologia Dr. Gama Pinto; the Health Research Institute-Fundación Jiménez Díaz University Hospital; Universidad Autónoma de Madrid; Massachusetts General Brigham IRB; and the University of Punjab, Lahore, Pakistan. Blood samples were collected from affected individuals and available family members after obtaining their written informed consent to participate in our study.

Study cohorts and analysis

Whole-genome sequence (WGS) data of individuals from a large UK cohort (Genomics England 100,000 Genomes Project[4] [UK100k][1] were analyzed to uncover the underlying cause of retinal degeneration in previously unresolved cases. In the UK100k main cohort, 2,316 participants (from 2,038 families) with inherited retinal degeneration (IRD) were recruited, with 35% of cases categorized as solved through the initial Genomics England variant analysis pipeline. This pipeline involved tiering of variants within relevant gene panels but did not initially include non-coding and structural variants. Scrutiny of genomic data from the unsolved UK100k IRD cohort included independent analysis of homozygous coding and noncoding rare variants (MAF < 0.01) across a panel comprising 216 retinal genes, known to be associated with either syndromic or non-syndromic retinal dystrophy (https://panelapp.genomicsengland.co.uk/panels/307/). The aim was to detect apparent homozygosity caused by heterozygous large deletions missed through the initial standard pipeline and to allow further scrutiny of variants of interest. Conducting case-specific analysis within the Genomics England's Interactive Variant Analysis (IVA) tool enabled each variant to be viewed across the whole UK100k rare disease cohort, alongside zygosity and key phenotypic information for each participant listed.

Independently, while the UK cohort screen was underway, a homozygosity mapping approach was used to study two consanguineous RP-affected families of Pakistani origin (A-4 and A-5) (Figures 1R and 1S). Prior to this analysis, these two families were unsolved as no likely causal/pathogenic coding sequence variants in known IRD genes of MAF 0.1% had been identified after WGS analysis.[6]

To identify additional RP-affected individuals with the two novel candidate causative *TMEM216* variants detected in the UK100k cohort and the two Pakistani families (A-4 and A-5), 5,930 molecularly uncharacterized RP-affected individuals at five additional centers were tested either by reviewing their NGS data or by targeted DNA sequencing: Ocular Genomics Institute, Massachusetts Eye and Ear, Boston, MA, USA (800 probands from 800 families); the University of Punjab, Lahore, Pakistan (215 affected individuals from 194 families); the Institute of Molecular and Clinical Ophthalmology Basel, Basel, Basel-Stadt, Switzerland (2,738 affected individuals from 2,703 families); the Health Research Institute-Fundación Jiménez Díaz University Hospital, Universidad Autónoma de Madrid (2,013 probands from 2,013 families); and the NIHR Bioresource for Rare Disease[1] at Moorfields Eye Hospital, London (NIHRRD) and the UK Inherited Retinal Disease Consortium (IRDC), London, UK (164 probands from 164 families).

Homozygosity mapping

Genome-wide homozygosity mapping of families A-4 and A-5 (Figures 1R and 1S) was performed as previously described using WGS data.[30,31] Briefly, homozygosity was calculated from common SNPs and indels with MAF >1%. For each individual, a data frame with the genomic position of all genotyped SNVs and a binary variable representing all heterozygous and homozygous alternative SNVs was constructed. The *smooth.spline* function with default parameters in R was used to calculate the frequency of homozygous and heterozygous SNPs. A stretch of homozygosity was defined if the smoothed frequency was <0.1% in at least 10,000 consecutive SNVs.

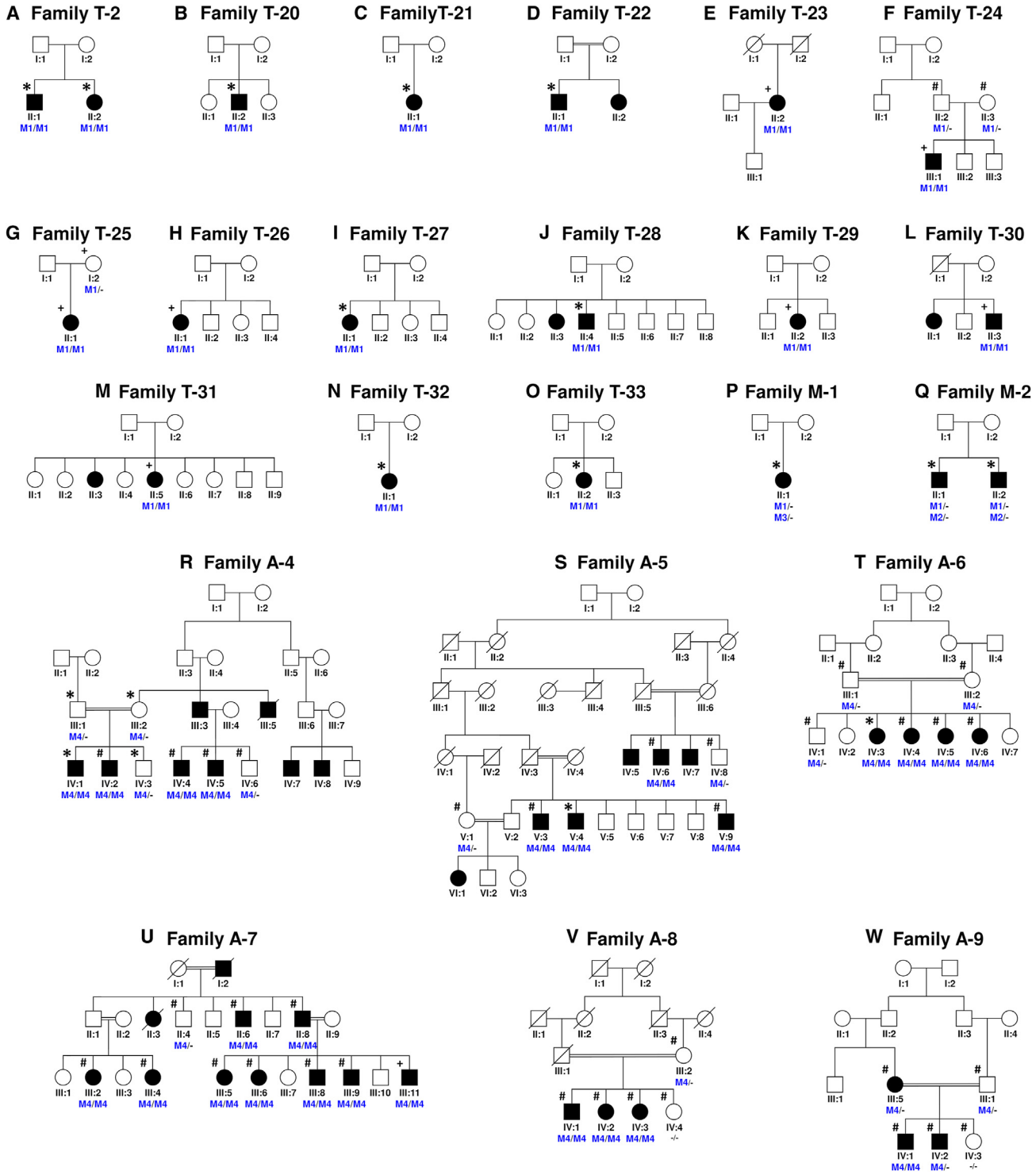

Figure 1. Segregation of *TMEM216* variants

Segregation analysis of *TMEM216* upstream sequence variants in representative pedigrees of African (A–Q) and South Asian (R–W) origin. M1, c.−69G>T; M2, g.61382891_61393975del; M3, c.35−2A>G; M4, c.−69G>A. *, +, and # indicates individuals that underwent whole-genome sequencing, whole-exome sequencing, or targeted sequencing, respectively. Consanguinity was present in all six pedigrees (family A4, A5, A6, A7, A8, and A9) of South Asian origin carrying M4, while detected in only one family of African origin (family T-22) carrying M1. Additional details of pedigrees are in Table 1.

The homozygosity mapping for families T-24, T-23, A-6, and A-7 (Figures 1E, 1F, 1T, and 1U) was performed using AutoMap with default parameters on whole-exome sequencing (WES) data (Figure S2).[32]

Haplotype analysis

Haplotypes of affected individuals carrying *TMEM216* (GenBank: NM_001173991.3) c.−69G>T or c.−69G>A alleles were constructed from SNPs at 50 kb intervals 1 Mb upstream and

downstream of the variant on chromosome 11 (g.60392563–62392563 [GRCh38]). The shared haplotype was identified by inspection in each group and was used to estimate the frequency of that haplotype in the corresponding population based on the 1000 Genomes database for the Punjabis in Lahore (PJL) chromosome 11 dataset for the Pakistani individuals and the combined Esan in Nigeria (ESN), Gambian in Western Division (GWD), Luhya in Webuye, Kenya (LWK), and Yoruba in Ibadan, Nigeria (YRI) datasets for the African individuals. Haplotype estimations were done by the EM (expectation maximization) and CHM (composite haplotype method) algorithms as incorporated in the Golden Helix SVS (SNP & Variation Suite) using default variables except that the minimum haplotype frequency was set to 0.0001 and a maximum of 100 EM iterations were allowed in order to predict accurate frequencies for rare haplotypes such as the risk haplotype conserved among all individuals homozygous for the causative g.61392563G>A and G>T alleles on chromosome 11. rs572262418 and rs760001653 were not found in the Pakistani and African 1000 Genomes datasets, respectively, probably due to a combination of low frequency of the rs572262418 minor allele in the Pakistani population and different frequencies of rs760001653 alleles in the various African populations included in the 1000 Genomes datasets. Because of this they were excluded from the haplotype analysis. This should not affect the haplotype frequency estimation as they are in complete linkage disequilibrium with the remaining SNPs in the risk haplotype in all affected individuals.

Clinical evaluation of affected individuals

All available participants underwent a full ophthalmic examination with a detailed clinical and family history. Retrospective clinical data were also gathered where available. Ophthalmic examination included visual acuity (Snellen and/or logMAR) and slit-lamp examination. Imaging included spectral domain optical coherence tomography (Spectralis, Heidelberg Engineering Ltd), ultra-widefield (UWF) color fundus photography (200°, Optos plc), and fundus autofluorescence (FAF) imaging, performed with 55° Spectralis or UWF Optos. Electrophysiological testing, when performed, included full-field and pattern electroretinography (ERG), which incorporated the International Society for Clinical Electrophysiology of Vision (ISCEV) standards.[33] The centers where the clinical evaluation of pedigrees was performed are listed in Table S1.

Impact of *TMEM216* c.−69 G>A and G>T variants on transcription factor binding

The Find Individual Motif Occurrences (FIMO) tool (MEME Suite 5.5.4) was used to scan a set of sequences for individual matches to motifs provided from JASPAR and HOCOMOCO databases.[34–36] Transcription factor (TF) positional weight matrices (PWMs) are used as input, and motif occurrences with a p value less than 0.001 were retained and analyzed.

Luciferase reporter gene assay

A genomic fragment spanning the *TMEM216* 5′ untranslated region (5′ UTR) and upstream non-coding sequence on chromosome 11 (g.61391712–61392642 [GRCh38]) was chosen for dual reporter luciferase assays. The fragment was chosen because of overlap with known retinal *cis*-regulatory elements (CREs) found in previous studies.[37] Six constructs were designed: wild-type, two versions harboring the variants c.−69G>A or c.−69G>T, and two constructs that removed predicted promoter 1 or 2, and a promoterless sequence (Table S3). The gene fragments were generated commercially (Twist Bioscience) and cloned (Gibson Assembly cloning Master Mix, New England Biolabs) into a modified version of the psiCHECK2 luciferase vector (Promega) lacking the SV40 promoter. The resulting plasmids were validated by Sanger sequencing and transfected into WERI-Rb1 cells (ATCCHTB-169) using X-tremeGENE HP DNA Transfection Reagent (Roche) according to the manufacturer's guidelines. Each experimental condition was tested in 10 biological replicates. Forty-eight hours post-transfection, luciferase assay was performed (Dual-Glo Luciferase assay, Promega) with luminescence reading performed by a plate spectrophotometer (SpectraMaxM3, Molecular Devices). Raw data were processed by subtracting the background luminescence of the un-transfected cell samples, normalization of the test renilla luciferase activity with the background firefly luciferase activity, and normalization with the wild-type construct. A promoterless construct served as a negative control. Statistical significance was assessed using Brown-Forsythe and Welch ANOVA and Dunnett's multiple comparison test (compared all groups against control group).

Expression of *TMEM216* and *TMEM138* in blood cells of individuals with *TMEM216* c.−69G>T

RNA was isolated from individuals homozygous for *TMEM216* c.−69G>T (T-23 and T-24) and unaffected control subjects from blood samples collected in Tempus Blood RNA tube (Thermo Fisher) and extracted using the Tempus Spin RNA isolation kit (Thermo Fisher). The extracted RNA was then purified using RNA cleanup and concentration kit (Qiagen) and converted into cDNA using the MultiScribe, High-Capacity cDNA Reverse Transcription Kit (Applied Biosystems). qPCR was performed on 4 ng of cDNA in 20 μL reactions with Fast-SYBR Green (4385612, Roche). Cycle threshold (CT) values were normalized using *GAPDH* (MIM: 138400) expression, and relative expression was calculated using 2-ΔΔCT method.[38] The experiment was repeated in triplicate using the same cDNA samples on the same day (experimental replicates). The primers used are listed in Table S1. For statistical analysis, two-tailed t test was performed.

Sequencing of *TMEM216* transcript from blood samples of individuals with *TMEM216* c.−69G>T

PaxGene blood samples were collected from an affected individual homozygous for c.−69G>T, unaffected carrier parent, and an unaffected control. Total RNA was purified using the PaxGene extraction kit (Qiagen) followed by reverse transcription to cDNA using random hexamers and SuperScript IV reverse transcriptase (Invitrogen). PCR was performed using primers designed to capture the canonical transcript (GenBank: NM_001173991.3) from exon 1 to –3′ UTR (Table S1). PCR product was purified (Ampure XP, Beckman Coulter Inc.). Up to 30 fmol of amplicon (Qubit High Sensitivity dsDNA quantification) was used for end preparation (Ultra II end-prep kit; NEB) and native barcoding (Oxford Nanopore Technologies; ONT: EXP-NBD104). Barcoded samples were pooled for library preparation (ONT ligation sequencing kit SQK-LSK110 Flongle protocol). Libraries were sequenced for 12 h using the Flongle flowcell and MinION sequencer.

Base calling was performed using the high-accuracy base calling mode in Minknow. Adaptor sequences were removed using

Porechop v.0.2.4,[39] and reads were filtered using NanoFilt v.2.8.0[40] for reads 800 to 1,800 bp with a quality score ≥ Q10. Resulting FastQ data were aligned to the human reference genome (build GRCh38) using minimap2 v.2.22.[41] BAM files were generated using SAMtools v.1.9.[42] The Integrative Genome Viewer[43] v.2.7.2 and v.2.14.1 were used to visualize aligned long reads. The heterozygous coding SNV present in the carrier parent (c.264G>A [p.Pro88Pro]) was used to visualize the relative amplification of the c.−69G vs. c.−69T alleles.

Generation of cell lines with *TMEM216* c.−69G>A

The hTERT-RPE1 cells (CRL-4000, ATCC) were used to generate the cell lines harboring the *TMEM216* c.−69G>A variant using two sets of sgRNAs and donor oligo sequences (Table S2) performed by Synthego. The cells were screened for the *TMEM216* c.−69G>A variant using PCR amplification and sequencing with the primers listed in Table S2.

Analysis of gene expression in hTERT-RPE1 cells with *TMEM216* c.−69G>A

The relative expression of *TMEM216* and *TMEM138* transcripts was studied in the WT and genome-edited hTERT-RPE1 cells with the *TMEM216* c.−69G>A variant in the homozygous or heterozygous state using primers listed in Table S2. Total mRNA was isolated from these cells, treated with RNase-free DNase, and purified using Qiagen RNeasy Mini Kit (Qiagen). Preparation of cDNA and RT-qPCR analyses were performed as described earlier.[44] The relative quantity was normalized to the expression levels of housekeeping genes *GAPDH* and *ACTB* (MIM: 102630) presented on an arbitrary scale to represent the relative levels of expression. The statistical significance (p value) was calculated using Student's t test as described previously.[44]

Evaluation of cilia in hTERT-RPE cells with *TMEM216* c.−69G>A

Genome-edited hTERT-RPE1 cells carrying *TMEM216* c.−69G>A variant in the heterozygous and homozygous states along with wild-type hTERT-RPE1 cells were studied using two independent clones of each genotype. These hTERT-RPE1 cells were cultured under serum-starved conditions and stained with acetylated α-tubulin antibodies (sc-23950, 1:200, Santa Cruz Biotechnologies) after 24 h of plating. Images were captured using Nikon confocal microscope system (A1R STORM). The ciliary phenotype was compared relative to the ciliary marker acetylated-α-tubulin. ImageJ64 software was used for measuring the number of the cilia in >200 cells for all genotypes in all clones.

Results

Identification of *TMEM216* c.−69G>T in individuals with retinitis pigmentosa that lack molecular diagnosis

One individual with simplex, non-syndromic retinitis pigmentosa, unsolved through the UK100k WGS analysis pipeline, was queried for apparent homozygous rare variants (MAF < 0.001) across a panel of 216 retinal dystrophy genes. 24 autosomal rare homozygous variants were found, none of which were homozygous in other individuals with retinal dystrophy across the entire UK100k cohort, with the exception of *TMEM216* c.−69G>T on chromosome 11 (g.61392563G>T [GRCh38], GenBank: NM_001173991.3). Analysis of the entire UK100k dataset identified 48 heterozygous and 18 apparent homozygous variant calls for this variant (Table 1). All 18 homozygotic individuals from 14 unrelated families had a clinical diagnosis of RP and remained undiagnosed through prior analysis. Zygosity of the apparent homozygotes was checked by inspection of trio genome segregation data and individual read data using IGV. Two affected siblings from one additional family (M-2) showed hemizygosity for the variant and a deletion in *trans*, encompassing exons 1–3 of *TMEM216* and much of the intergenic region distal to *TMEM138* upstream of the gene on chromosome 11 (g.61,382,891–61,393,975 [GRCh38]) (Figure 1Q).

An additional 24 individuals homozygous for *TMEM216* c.−69G>T were identified across 24 families following genetic analysis of 5,874 families with 5,930 unsolved IRD cases from additional cohorts. One further individual (M-1) was a compound heterozygote for this and *TMEM216* c.35−2A>G on chromosome 11 (g.61393229A>G [GRCh38]), a previously reported pathogenic variant (Figure 1P).[2] All 45 individuals from 40 families were of either African (Zimbabwe, Ghana, Nigeria, Angola), Caribbean (Jamaica, Barbados, Haiti), or African American descent (Figures 1A–1Q; Table 1). The variant has an allele frequency (AF) of 0.0002739 (407/1,485,934 alleles) in the gnomAD v4 dataset with enrichment in the African/African American genetic ancestry group (362/71,782 alleles, AF: 0.005043) including one homozygote, but was completely absent in non-Finnish European individuals (1,105,112 alleles).[45]

Identification of *TMEM216* c.−69G>A in individuals with RP

In 2021, Biswas et al. performed whole-genome sequencing in 108 unrelated pedigrees from three different ethnic populations.[6] The WGS data from nine members of two consanguineous Pakistani families with RP that were not solved by the latter study (A-4 and A-5, Figures 1R and 1S) were subjected to a careful search for homozygous regions of the genome that segregated with the disease phenotype. This analysis revealed a ∼8.25 Mb homozygous region on chromosome 11 (g.55,000,000–63,258,298) shared by the three affected individuals of A-4 (IV:2, IV:4, and IV:5 in Figure 1R; Figure 2A). This homozygous region is also partially shared with one affected individual (V:4 in Figure 1S) from the second family, A-5. Among all four affected individuals, the stretch of homozygosity overlapped, and the size of the shared region was 1.57 Mb on chromosome 11 (g.61,145,940–62,715,657).

Analysis of all rare variants within this shared homozygous region and segregation analysis of additional family members revealed a rare non-coding homozygous variant, *TMEM216* c.−69G>A on chromosome 11 (g.61392563G>A [GRCh38], GenBank: NM_001173991.3). This variant segregated with RP in both pedigrees (Figures 1R and 1S) and was found in the gnomAD v4 dataset with a frequency of 0.00005855 (87/1,485,932 alleles), with enrichment in the

Table 1. Summary of demographic information and clinical phenotype of selected affected individuals from African and South Asian families with *TMEM216* variants

Family ID	*TMEM216* genotype	Figure 1 identifier	Ethnicity	Gender	Known consanguinity	Reported age of onset	Ophthalmology phenotype	Non-ophthalmology phenotype	Most recent VA (best corrected RE)	Most recent VA (best corrected LE)
T-1	HOM c.−69G>T	NS	black African (Nigeria)	M	no	4 years	BE RP with unusual asymmetry; sudden loss of LE vision at 12 years; LE squint and cataract	None	CF	NPL
T-2a	HOM c.−69G>T	A	black African (Nigeria)	F	no	4 years	BE RP; intermittent divergent squint; myopia	pre-term infant	20/30	20/25
T-2b	HOM c.−69G>T	A	black African (Nigeria)	F	no	4 years	BE RP; cystoid macular edema; myopia	none	20/60	20/60
T-3	HOM c.−69G>T	NS	black African (Nigeria)	M	no	5 years	BE RP; RE marginal cystoid macular edema	none	1/60	2/60
T-4	HOM c.−69G>T	NS	black Caribbean (Barbados)	F	no	3 years	BE RP; myopia	balance problems	20/60	20/60
T-5	HOM c.−69G>T	NS	black African	M	no	childhood	BE RP; BE macular edema	none	20/60	20/120
T-6	HOM c.−69G>T	NS	black African (Zimbabwe)	F	no	4 years	BE RP; BE pseudophakia; BE macular edema	none	20/30	20/40
T-7a	HOM c.−69G>T	NS	black African (Nigeria)	F	no	childhood	BE RP	Hashimotos; thyroid problems; clotting disorder	20/32	20/32
T-7b	HOM c.−69G>T	NS	black African (Nigeria)	M	no	childhood	BE RP	none	–	–
T-8	HOM c.−69G>T	NS	black Caribbean (Jamaica) and black African	F	no	3 years	BE RP	autism	20/40	20/40
T-9a	HOM c.−69G>T	NS	black Caribbean (Jamaica and Barbados)	M	no	childhood	BE RP	none	20/50	20/40
T-9b	HOM c.−69G>T	NS	black Caribbean (Jamaica and Barbados)	M	no	early childhood	BE RP	none	20/30	20/20
T-10	HOM c.−69G>T	NS	black African	F	no	early childhood	BE RP	none	20/25	20/25
T-11	HOM c.−69G>T	NS	black African	F	no	childhood	BE RP	none	CF	20/200
T-12	HOM c.−69G>T	NS	black African (Zimbabwe)	F	no	5 years	BE RP	none	20/50	20/50
T-13	HOM c.−69G>T	NS	black African (Nigeria)	F	no	childhood	BE RP; myopia	none	20/40	20/32
T-14	HOM c.−69G>T	NS	black African (Nigeria)	F	no	childhood	BE RP	none	20/200	20/200

(*Continued on next page*)

Table 1. ***Continued***

Family ID	*TMEM216* genotype	Figure 1 identifier	Ethnicity	Gender	Known consanguinity	Reported age of onset	Ophthalmology phenotype	Non-ophthalmology phenotype	Most recent VA (best corrected RE)	Most recent VA (best corrected LE)
T-15a	HOM c.−69G>T	NS	black African	F	N/A	N/A	BE RP	none	N/A	N/A
T-15b	HOM c.−69G>T	NS	black African	F	N/A	N/A	BE RP	None	N/A	N/A
T-16	HOM c.−69G>T	NS	black African	M	N/A	N/A	BE RP	None	N/A	N/A
T-17	HOM c.−69G>T	NS	black Caribbean	F	N/A	N/A	BE RP	significant early-onset obesity	N/A	N/A
T-18	HOM c.−69G>T	NS	black African	M	N/A	N/A	BE RP	none	N/A	N/A
T-19	HOM c.−69G>T	NS	black African	F	N/A	N/A	BE RP	none	N/A	N/A
T-20	HOM c.−69G>T	B	black African (Nigeria)	M	no	6 years	BE RP	none	20/20	20/20
T-21	HOM c.−69G>T	C	black African (Nigeria)	F	no	early childhood	BE RP; LE strabismus	Aspergers	20/40	20/60
T-22	HOM c.−69G>T	D	black African	M	no	childhood	BE RP	none	20/40	20/60
T-23	HOM c.−69G>T	E	black Caribbean (Haiti)	F	no	early childhood	BE RP	none	LP	LP
T-24	HOM c.−69G>T	F	African (Angola)	M	no	childhood	BE RP; myopia	none	20/25	20/25
T-25	HOM c.−69G>T	G	African American	F	no	19 years	BE RP; RE cystoid macular edema; high myopia; BE presbyopia	none	20/60−2	20/40+2
T-26	HOM c.−69G>T	H	African American	F	no	8-9 years	BE RP	none	20/30	20/30
T-27	HOM c.−69G>T	I	black Caribbean	F	no	5 years	BE RP; RE amblyopia	none	CF	20/50
T-28	HOM c.−69G>T	J	black Caribbean	M	no	12 years	BE RP	none	20/200+1	20/200
T-29	HOM c.−69G>T	K	African American	F	no	6 years	BE RP; high myopia	none	20/40	20/200
T-30	HOM c.−69G>T	L	African American	M	no	9 years	BE RP	none	20/20	20/25
T-31	HOM c.−69G>T	M	black Caribbean (Jamaica)	F	no	43 years	BE RP; BE small posterior subcapsular cataracts	none	20/80	20/400
T-32	HOM c.−69G>T	N	African American	F	no	5 years	BE RP	none	20/400	20/200
T-33	HOM c.−69G>T	O	African (Algeria)	F	no	childhood (nyctalopia)	BE RP	none	20/40	20/40
T-34	HOM c.−69G>T	NS	black African	M	no	3 years	BE RP; macula edema	none	20/32	20/30
T-35	HOM c.−69G>T	NS	black Caribbean	F	no	5 years	BE RP	none	20/32	20/20
T-36	HOM c.−69G>T	NS	black Caribbean	M	no	childhood	BE RP; LE Fuch's heterochromic cyclitis	none	20/125	20/200
T-37	HOM c.−69G>T	NS	black African (Ghana)	F	no	childhood	BE RP	none	20/30	20/30

(*Continued on next page*)

Table 1. *Continued*

Family ID	*TMEM216* genotype	Figure 1 identifier	Ethnicity	Gender	Known consanguinity	Reported age of onset	Ophthalmology phenotype	Non-ophthalmology phenotype	Most recent VA (best corrected RE)	Most recent VA (best corrected LE)
T-38	HOM c.−69G>T	NS	African	F	N/A	N/A	BE RP	none	N/A	N/A
M-1	HET c.−69G>T, HET c.35−2A>G	P	black Caribbean	F	no	3 years	BE RP; BE macular hole; myopia	none	20/200	20/40
M-2a	HET c.−69G>T, HET deletion*	Q	black African (Zimbabwe)	M	no	6 years	BE RP; BE pseudophakia; myopia	none	20/30	20/30
M-2b	HET c.−69G>T, HET deletion*	Q	black African (Zimbabwe)	M	no	6 years	BE RP	none	N/A	N/A
A-1a	HOM c.−69G>A	NS	Pakistani	M	yes	5 years	BE RP	right hemiplegia; epilepsy	20/40	20/60
A-1b	HOM c.−69G>A	NS	Pakistani	M	yes	early childhood	BE RP	none	20/25	20/20
A-2	HOM c.−69G>A	NS	Bangladeshi	M	yes	childhood	BE RP	none	20/63	20/40
A-3	HOM c.−69G>A	NS	Pakistani	F	yes	childhood	BE RP; BE early central posterior subcapsular cataract	none	20/25	20/25
A-4a	HOM c.−69G>A	R	Pakistani	M	yes	5–8 years	BE RP	none	N/A	N/A
A-4b	HOM c.−69G>A	R	Pakistani	M	yes	5–8 years	BE RP	none	N/A	N/A
A-4c	HOM c.−69G>A	R	Pakistani	M	yes	5–8 years	BE RP	none	N/A	N/A
A-4d	HOM c.−69G>A	R	Pakistani	M	yes	5–8 years	BE RP	none	N/A	N/A
A-5a	HOM c.−69G>A	S	Pakistani	M	yes	5–10 years	BE RP	none	N/A	N/A
A-5b	HOM c.−69G>A	S	Pakistani	M	yes	5–10 years	BE RP	none	N/A	N/A
A-5c	HOM c.−69G>A	S	Pakistani	M	yes	5–10 years	BE RP	none	N/A	N/A
A-5d	HOM c.−69G>A	S	Pakistani	M	yes	5–10 years	BE RP	none	N/A	N/A
A-5e	HOM c.−69G>A	S	Pakistani	F	yes	5–10 years	BE RP	none	N/A	N/A
A-6	HOM c.−69G>A	T	Pakistani	F	yes	childhood	BE RP	none	N/A	N/A
A-7	HOM c.−69G>A	U	Pakistani	M	yes	childhood	BE RP	none	20/200	20/160
A-8	HOM c.−69G>A	V	Pakistani	F	yes	1–3 years	BE RP	none	N/A	N/A
A-9	HOM c.−69G>A	W	Pakistani	M	yes	5–8 years	BE RP	none	N/A	N/A

Demographics, pedigree, and phenotype information obtained where available. Lowercase in family ID represent members of the same family. "Age of onset" as reported by subject of earliest signs of nyctalopia or vision loss. Ethnicity data gathered as reported by subject. Visual acuities converted to imperial Snellen scale. *Heterozygous deletion of g.61,382,891–61,393,975 (GRCh38) on chromosome 11 found in *trans* with *TMEM216* c.−69G>T. HOM, homozygous; HET, heterozygous; YOB, year of birth; F, female; M, male; BE, both eyes; RE, right eye; LE, left eye; RP, retinitis pigmentosa; VA, visual acuity; CF, counting fingers; NPL, no perception of light; LP, light perception; N/A, not available; NS, not shown in Figure 1.

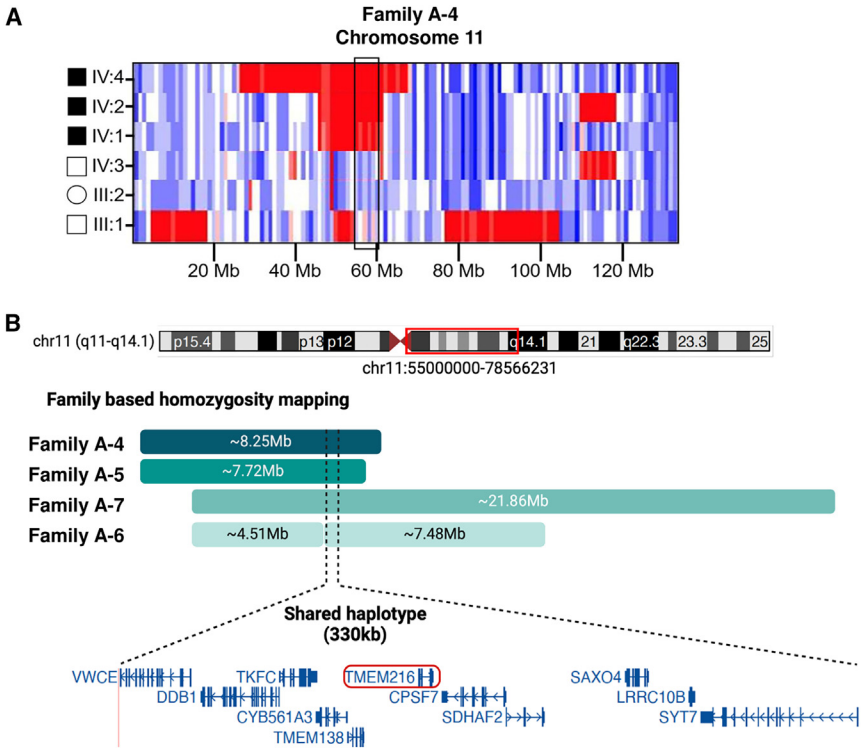

Figure 2. Homozygosity mapping of family A-4 and across families with *TMEM216* c.−69G>A

(A) Homozygosity in affected and unaffected members of A-4 across the genome identified an 8.25 Mb (g.55,000,000–63,258,298 [GRCh38]) region on chromosome 11 shared by three affected individuals. Red indicates variants in the region that are homozygous, blue indicates alleles that are heterozygous, and white indicates homozygous and heterozygous alleles in the same frequency.

(B) Homozygosity mapping across families with *TMEM216* c.−69G>A: homozygous regions identified on chromosome 11 in pedigrees A-4, A-5, A-7, and A-6 and 11 genes located within the 330 kb shared homozygous interval are shown.

South Asian genetic ancestry group (79/82,738 alleles, AF: 0.0009548).[45]

Analysis of the genomic data of 315 additional pedigrees with affected individuals that remained without molecular diagnosis after WGS or WES analysis out of a total of ∼716 unrelated IRD-affected pedigrees recruited from Pakistan resulted in the identification of *TMEM216* c.−69G>A in the homozygous state in affected individuals from two additional families: A-6 and A-7. Examination of the homozygous regions identified in individuals from these two families narrowed the shared homozygous interval to 330 kb (Figure 2B).

Further, targeted variant analysis of affected individuals from additional Pakistani pedigrees by Sanger sequencing revealed the presence of the *TMEM216* c.−69G>A variant in the homozygous state in affected individuals from two pedigrees, A-8 and A-9 (Figures 1V and 1W). This variant segregated in the homozygous state with RP in one family (A-8) while in the second family (A-9), one affected member had the variant in the homozygous state and two other affected members carried this variant in the heterozygous state (Figures 1V and 1W). The underlying cause of disease in these heterozygous carriers that lacked potentially pathogenic variants in other genes including TMEM216 remains unknown and may be independently inherited.

Subsequent screening of the datasets of UK100k and NIHRRD cohorts identified four additional RP-affected individuals from three families (A-1, A-2, and A-3) of South Asian origin, homozygous for *TMEM216* c.−69G>A (Table 1). In summary, the homozygous *TMEM216* c.−69G>A variant was observed in affected individuals from 9 families of South Asian origin with a clinical diagnosis of RP and no molecular diagnosis (Figures 1R–1W; Table 1).

Haplotype mapping

Haplotypes formed by SNPs selected for having a minimum fraction of heterozygotes in the gnomAD database for that particular population (African and South Asian) of 0.3 in the *TMEM216* region on chromosome 11 of affected individuals were assembled in the Pakistani and African individuals and extended from *TMEM216* c.−69G (g.61392563) until at least one haplotype in each group diverged (Table 2). In the African affected individual group, the shared haplotype extends 177 kb from rs61895905 on chromosome 11 (g.61340630) to rs3019201 (g.61517826). In the Pakistani individuals, it spans 330 kb from rs373641413 (g.61264929) to rs79136768 (g.61594967) on chromosome 11 (Table 3). These two conserved haplotypes strongly suggest a single founder mutation unique to each group. The conserved haplotypes were not found in the predicted haplotype sets for either the Pakistani or African population groups, so the 1000 Genomes datasets were seeded with a single homozygous carrier for the shared founder haplotype to give a conservative upper limit for the frequency. The estimated population frequencies for the shared haplotypes when the single carriers are included are 0.01 for the Pakistani population and 0.0023 for the African population giving a $p < 1.3 \times 10^{-18}$ and $p < 3.6 \times 10^{-53}$ for a single founder mutation for the Pakistani and African population, respectively.

All individuals with the c.−69G>A variant were from consanguineous unions while all with the c.−69G>T variant did not report consanguinity (Table 1). This is exemplified by high total size of regions of homozygosity (ROHs) in the four families with c.−69G>A and low total size of ROHs in the two families with c.−69G>T (Figures 2 and S2). Individuals reporting consanguinity typically have more than 100 Mb of total size of ROHs.

Table 2. Conserved region of homozygosity across *TMEM216* c.−69G>T in African families

rsID	rs28720354	rs61895905	rs760001653	rs73492397	rs563641208[a]	rs3018731	rs2943813	rs2957857	rs56408067	rs3017596	rs2924439	rs3019201	rs441938
Variant (chr11)	61301 517G>A	613406 30A>G	613785 64G>A	613903 67T>G	613925 63G>T	614813 04A>G	614909 96T>C	614940 45G>A	614975 60G>A	61505 678T>G	615139 58G>A	615178 26G>C	61549 915G>A
Distance from 613925 63G>T (bp)	91,046	51,933	13,999	2,196	–	88,741	98,433	101,482	104,997	113,116	121,395	125,263	157,352
gnomAD AF (African)	0.1577	0.7105	0.3697	0.1628	0.005043	0.5173	0.3539	0.6024	0.495	0.5755	0.4414	0.1402	0.161
Shared haplotype (177 kb)													
Family ID	Genotype												
T-3	A/A	A/A	A/A	G/G	T/T	G/G	C/C	A/A	A/A	G/G	A/A	C/C	G/G
T-5	A/A	A/A	A/A	G/G	T/T	G/G	C/C	A/A	A/A	G/G	A/A	C/C	G/G
T-2	A/A	A/A	A/A	G/G	T/T	G/G	C/C	A/A	A/A	G/G	A/A	C/C	G/G
T-4	A/A	A/A	A/A	G/G	T/T	G/G	C/C	A/A	A/A	G/G	A/A	C/C	G/G
T-15	A/A	A/A	A/A	G/G	T/T	G/G	C/C	A/A	A/A	G/G	A/A	C/C	G/G
T-6	A/A	A/A	A/A	G/G	T/T	G/G	C/C	A/A	A/A	G/G	A/A	C/C	G/G
T-16	A/A	A/A	A/A	G/G	T/T	G/G	C/C	A/A	A/A	G/G	A/A	C/C	G/G
T-7	A/A	A/A	A/A	G/G	T/T	G/G	C/C	A/A	A/A	G/G	A/A	C/C	G/G
T-1	A/A	A/A	A/A	G/G	T/T	G/G	C/C	A/A	A/A	G/G	A/A	C/C	G/G
T-8	A/A	A/A	A/A	G/G	T/T	G/G	C/C	A/A	A/A	G/G	A/A	C/C	G/G
T-17	A/A	A/A	A/A	G/G	T/T	G/G	C/C	A/A	A/A	G/G	A/A	C/C	G/G
T-18	A/A	A/A	A/A	G/G	T/T	G/G	C/C	A/A	A/A	G/G	A/A	C/C	G/G
T-19	G/G	A/A	A/A	G/G	T/T	G/G	C/C	A/A	A/A	G/G	A/A	C/C	G/G
T-35	A/A	A/A	A/A	G/G	T/T	G/G	C/C	A/A	A/A	G/G	A/A	C/C	A/G
T-37	A/A	A/A	A/A	G/G	T/T	G/G	C/C	A/A	A/A	G/G	A/A	C/C	G/G
T-36	A/A	A/A	A/A	G/G	T/T	G/G	C/C	A/A	A/A	G/G	A/A	C/C	G/G
T-34	A/A	A/A	A/A	G/G	T/T	G/G	C/C	A/A	A/A	G/G	A/A	C/C	G/G
T-24	A/A	no data	no data	G/G	T/T	G/G	no data	no data	A/A	G/G	A/A	no data	G/G
T-23	A/A	no data	no data	no data	T/T	G/G	C/C	no data	A/A	G/G	A/A	C/C	G/G
T-27	A/A	no data	A/A	G/G	T/T	G/G	C/C	A/A	A/A	G/G	A/A	C/C	no data
T-28	A/A	no data	A/A	G/G	T/T	G/G	C/C	A/A	A/A	G/G	A/A	C/C	no data
T-32	A/A	no data	A/A	G/G	T/T	G/G	C/C	A/A	A/A	G/G	A/A	C/C	no data
T-33	A/A	no data	A/A	G/G	T/T	G/G	C/C	A/A	A/A	G/G	A/A	C/C	no data

Genotyping shown for selected African informative families, with only one individual in each family represented. AF, allele frequency.
[a]Putative disease variant

Table 3. Conserved region of homozygosity across *TMEM216* c.−69G>A in South Asian families

rsID	rs575542365	rs373641413	rs56358658	rs572262418	rs563641208[a]	rs571401170	rs78258051	rs2924440	rs441938	rs79136768	rs1692122
Variant (chr11)	61145940C>G	61264929G>A	61323113C>T	61333462A>G	61392563G>A	61455562C>A	61479807T>C	61513165G>A	61549915G>A	61594967A>G	61663516C>A
Distance from 61392563G>A (bp)	246,623	127,634	69,450	59,101	–	62,999	87,244	120,602	157,352	202,404	270,953
gnomAD AF (South Asian)	0.003107	0.0009561	0.0357	0.02762	0.02762	0.01988	0.04028	0.6408	0.4385	0.0951	0.7378
Shared haplotype (330 kb)											
Family ID	Genotype										
A-1	G/G	A/A	T/T	G/G	A/A	A/A	C/C	A/A	G/G	A/A	A/A
A-2	G/G	A/A	T/T	G/G	A/A	A/A	C/C	A/A	G/G	A/A	A/A
A-8	G/G	A/A	T/T	G/G	A/A	A/A	C/C	A/A	G/G	A/A	A/A
A-9	C/C*	A/A	T/T	G/G	A/A	A/A	C/C	A/A	G/G	A/A	A/A
A-6	G/G	A/A	T/T	G/G	A/A	A/A	C/C	A/A	G/G	A/A	C/C*
A-7	C/C*	A/A	T/T	G/G	A/A	A/A	C/C	A/A	G/G	A/A	A/A
A-5	G/G	A/A	T/T	G/G	A/A	A/A	C/C	A/A	G/G	A/A	C/C*
A-4	C/C*	A/A	T/T	G/G	A/A	A/A	C/C	A/A	G/G	A/A	C/C*

Genotyping shown for selected South Asian informative families, with only one individual in each family represented. * indicates discordant SNPs. AF, allele frequency.
[a]Putative disease variant

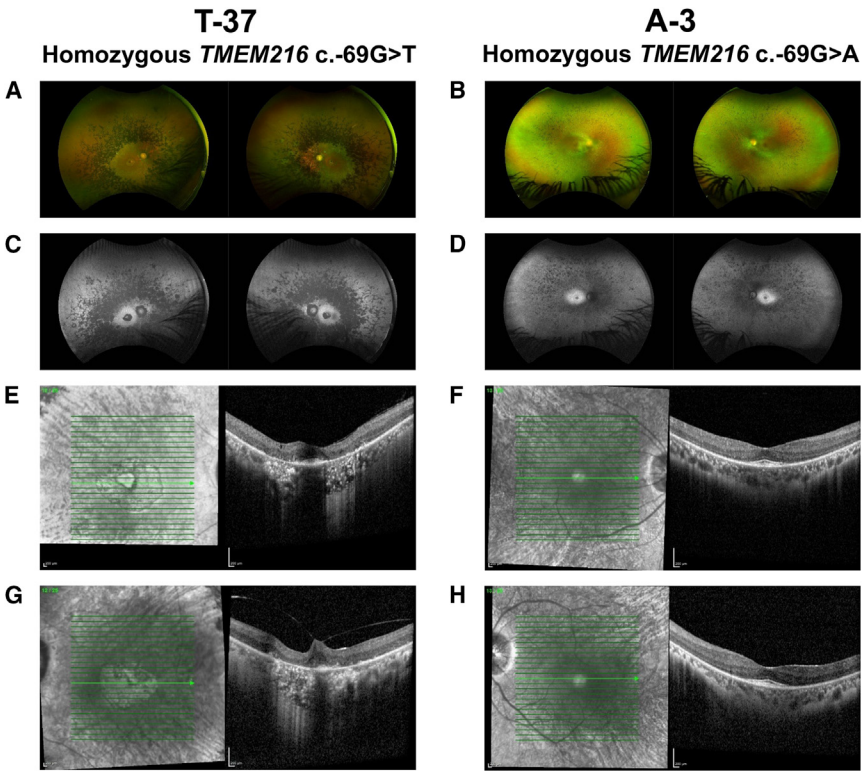

Figure 3. Clinical findings for individuals with *TMEM216* c.−69G>T and *TMEM216* c.−69G>A variants of 72 and 24 years of age, respectively

(A–D) *En face* pseudo color images (A and B) and green (532 nm) autofluorescence (C and D) from an Optos wide-angle fundus camera. The 72-year-old individual shows a greater amount of pigment and further reduction in autofluorescence (A and C). In the 24-year-old individual, there is typical bone-spicule pigment in the peripheral retina. This individual showed loss of autofluorescence, with retention of autofluorescence within a 10-degree area centered on the fovea (B and D).

(E–H) *En face* infrared and OCT images of the right (E and F) and left (G and H) eyes centered on the fovea. The 72-year-old individual showed atrophy of both outer retina and RPE on OCT with some preservation of the foveal layers. In the 24-year-old individual, the region of preserved retinal anatomy on OCT imaging matches the retained autofluorescence observed in (D) (F and H).

Clinical phenotype of subjects with *TMEM216* c.−69G>A and c.−69G>T

Of the bi-allelic *TMEM216* individuals, detailed clinical data were available for 31 seen at Moorfields Eye Hospital, London, UK (aged 9–73 years, 16 females/15 males) (Table 1). All had night blindness in the first decade of life, with progressive loss of peripheral field over subsequent decades. The childhood-onset night blindness resembled the clinical profile typically seen in individuals with RP consequent upon bi-allelic variants of genes involved in rod phototransduction such as *CNGB1* (MIM: 600724), *CNGA1* (MIM: 123825), *PDE6B* (MIM: 180072), and *PDE6A* (MIM: 180071). Foveal structure and function were initially preserved, with loss of acuity from the third decade. OCT and *en face* imaging were of typical RP in which there is primary loss of rod photoreceptor structure with secondary loss of the cone-rich central macula and fovea. Representative images are shown in Figure 3. Electrophysiology showed abrogated responses to both rod and cone stimuli using ISCEV standard conditions. Even at an early age (3 individuals were tested prior to 10 years of age), there were barely detectable cone-driven and undetectable rod-driven responses. There were no evident differences in the age of onset and progression of those with homozygosity for *TMEM216* c.−69G>T compared to *TMEM216* c.−69G>A, nor in the two mixed heterozygotes for *TMEM216* c.−69G>T. No evident systemic features suggestive of generalized ciliopathy were noted in affected persons (Table 1). Evaluation of affected members of other families with these non-coding variants showed a clinical course consistent with that described above.

c.−69G>A and c.−69G>T downregulate *TMEM216* expression *in vitro*

A dual reporter luciferase assay was performed to test whether the noncoding variants c.−69G>A and c.−69G>T alter *TMEM216* gene expression. The 931 bp test sequence contained the genomic sequence spanning the 5′ untranslated region (UTR) of *TMEM216* and upstream non-coding sequence on chromosome 11 (g.61,391,712–61,392,642 [GRCh38]) (Figure 4A). Two promoters were predicted in this region according to the Eukaryotic Promoter Database[46]: promoter 1 (P1, g.61,392,583–61,392,642 [GRCh38] on chromosome 11) overlapping with the *TMEM216* 5′ UTR (GenBank: NM_001173991.3) and an upstream promoter 2 (P2, g.61,392,331–61,392,390 [GRCh38] on chromosome 11). The region contains known retinal transcription factor binding sites (CRX and OTX2) and lies within an ATAC peak (Figure 4A).[37,46] FIMO transcription factor analysis using JASPAR TF motif PWMs predicted differential binding of transcription factors between wild-type and the sequence containing both variants.

Five constructs were tested: a reference and two variant constructs containing either the c.−69G>A or c.−69G>T variant and two deletion constructs with deletions involving individual predicted promoter sequences P1(ΔP1) and P2 (ΔP2) (Figure 4B). Both *TMEM216* c.−69G>A and c.−69G>T variants resulted in a significant downregulation of luciferase activity (26% and 36% of reference expression respectively, p value < 0.0001), suggesting a hypomorphic nature of these variants. A more pronounced downregulation was observed when the proximal promoter (P1) was missing (p value < 0.0001).

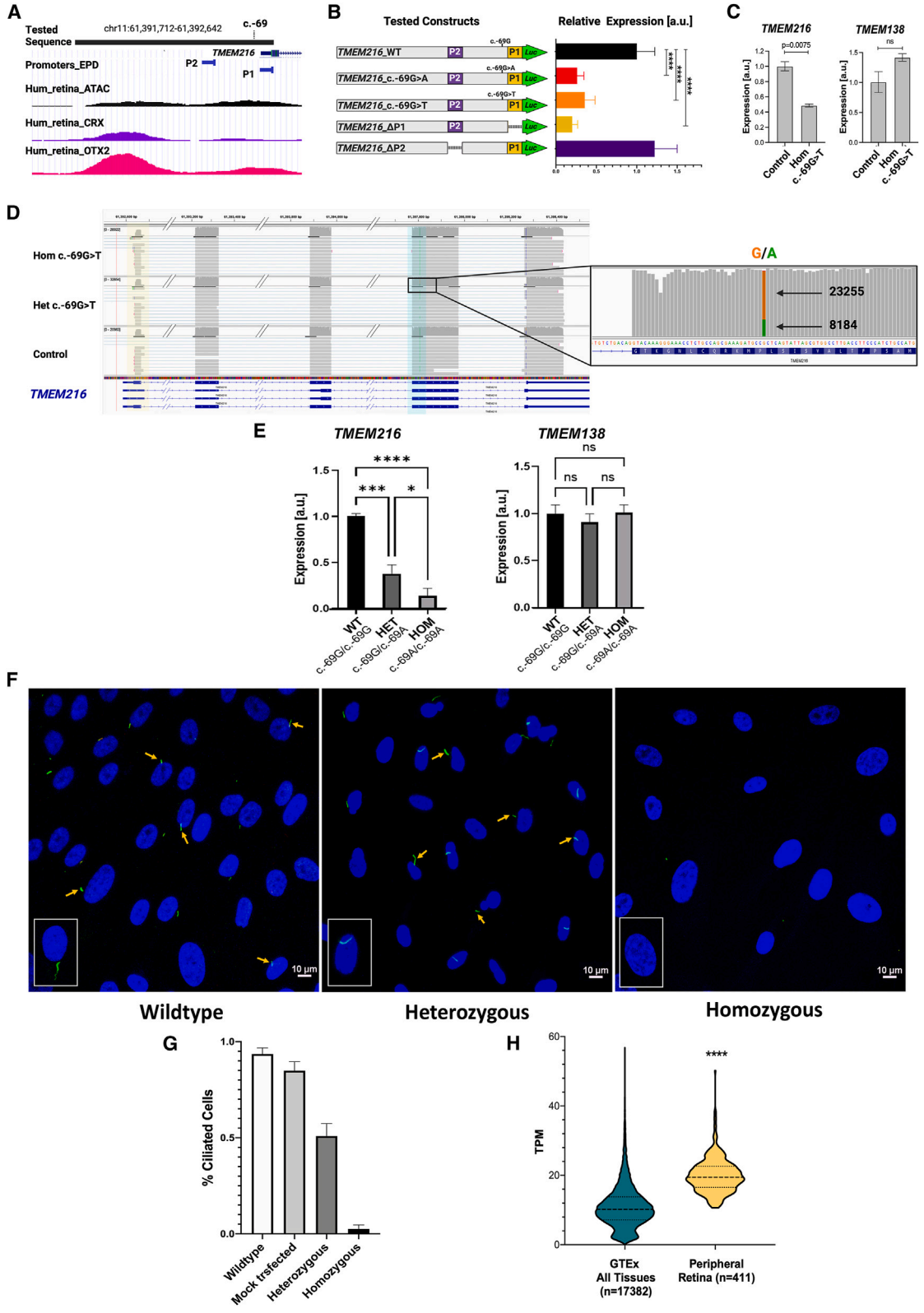

Figure 4. The c.−69 variants downregulate *TMEM216* expression *in vitro* and *in vivo*

(A) Characteristics of the 931-bp region upstream of *TMEM216* on chromosome 11 used in the luciferase assay (g.61,391,712–61,392,642 [GRCh38]). This 931-bp region contains *cis*-regulatory elements for known retinal transcription factors, such as CRX and OTX2, and two predicted promoter sequences (P1 and P2).[37,46]

(B) Relative luciferase activity for the reference and mutated constructs containing the *TMEM216* c.−69G>A, c.−69G>T, and additional constructs harboring deletions of the predicted P1 and P2 promoters. Luciferase activity was normalized by a construct with no promoter sequence and the WT control. ****$p < 0.0001$.

(legend continued on next page)

Deletion of the distal promoter (P2) did not show significant differences when compared to the reference construct (Figure 4B).

Reduced expression of *TMEM216* in leukocytes of individuals with *TMEM216* c.−69G>T

RT-qPCR was performed to analyze the expression levels of *TMEM216* and *TMEM138* in blood samples from the WT control subjects and affected individuals from pedigrees T-23 and T-24 homozygous for *TMEM216* c.−69G>T. The results revealed a significant reduction of 51% of *TMEM216* expression in homozygous compared to wild-type individuals (p value = 0.0075) (Figure 4C). However, no significant difference was observed in the expression of *TMEM138* in affected individuals compared to control subjects (Figure 4C).

Skewed allele balance in a c.−69G>T carrier

IGV read depth analysis of blood-derived *TMEM216* RT-chPCR transcripts using ONT single-molecule sequencing yielded 26,922 reads from a homozygous individual, 32,854 from a carrier individual, and 20,963 from a control subject (Figure 4D). The reads were phased in the carrier parent sample using the heterozygous SNV c.264G>A (A allele) in *cis* with the c.−69T allele. Reads covering this nucleotide position showed an allele balance of 74%/26% (23,255 reads/8,184 reads) of the c.−69G; c.264G allele to the c.−69T; c.264A allele, suggesting a relative reduction in transcription from the c.−69T allele.

The generation of two distinct isoforms from differential usage of the exon 1 donor site is shown in each of the samples with a similar ratio of long to short exon 1 3′ ends across samples (Figure 4D). Moreover, when examined separately, the mutant and wild-type alleles from the heterozygous parent (2nd row) showed exon 1 usage short:-long as follows: mutant, 5,106:962 (16% long); wild-type, 18,892:5,970 (24% long). Overall, these data would support the model that the c.−69G>T variant causes reduced but not abrogated expression.

Reduced expression of *TMEM216* in hTERT-RPE1 cells with *TMEM216* c.−69 G>A

hTERT-RPE1 cells were generated by introducing this variant using CRISPR-Cas9, which resulted in the generation of cell lines heterozygous and homozygous for this *TMEM216* c.−69G>A variant. Unfortunately, the cell line homozygous for the *TMEM216* c.−69G>A variant also had an additional variant *TMEM216* c.−71C>T (g.61392561C>T on chromosome 11) introduced during the gene editing process (Figure S1).

Compared to the control wild-type, the relative expression of *TMEM216* was reduced by 86.3% (p value < 0.001) in the genome-edited cells homozygous for c.−69G>A/c.−71C>T and by 62.1% (p value < 0.05) in cells heterozygous for c.−69G>A. These results indicate that *TMEM216* c.−69G>A lowers the expression of *TMEM216* (Figure 4E). However, the relative expression of *TMEM138* which is known to share a regulatory region with *TMEM216* was not altered based on the presence of the variant (Figure 4E).

The expression of three other IRD genes was also evaluated in these cells, due to their proximity to the *TMEM216* c.−69G>A variant. The *BEST1* (MIM: 607854), *ASRGL1* (MIM: 609212), and *ROM1* (MIM: 180721) genes located on chromosome 11 (55 kb, 95 kb, and 1.2 Mb away, respectively, from c.−69G>A) showed no significant difference in their expression between mutant and control hTERT-RPE1 cells (data not shown).

Abnormal ciliogenesis in hTERT-RPE1 cells with *TMEM216* c.−69 G>A

The ciliary morphology of hTERT-RPE1 cells carrying the c.−69G>A variant was evaluated as *TMEM216* deficiency is known to affect primary ciliogenesis.[47] Immunocytochemistry of hTERT-RPE1 cells with the ciliary marker acetylated tubulin antibodies revealed reduced ciliogenesis

(C) Real-time quantitative PCR quantification of *TMEM216* and the neighboring *TMEM138* gene expression in blood samples from two WT control subjects and two individuals carrying the homozygous *TMEM216* c.−69G>T variant (T-24 and T-23).
(D) IGV representation of cDNA reads from Oxford Nanopore sequencing of leukocyte RNA. Top lane, an affected individual homozygous for c.−69G>T; middle lane, the heterozygous mother; bottom lane, a healthy WT control subject. Red vertical line represents the variant base c.−69G, which is not included in the RNA sequence. The right panel shows the relative read depths for a benign coding SNV (rs3741265, c.264G>A [p.Pro88Pro]) for which the mother is heterozygous. The A allele, in *cis* with the c.−69G>T mutation, is represented at a significantly lower concentration than the G allele (read depth 8,184 [A] versus 23,255 [G]).
(E) RT-qPCR analysis of gene expression in hTERT-RPE1 cells. Quantitative PCR analysis of *TMEM216* and *TMEM138* expression across all three genotypes. Expression is relative to *GAPDH* housekeeping gene. One-way ANOVA results are shown (*p < 0.05, **p < 0.01, ***p < 0.001, ****p < 0.0001).
(F) Functional validation of *TMEM216* c.−69G>A in hTERT-RPE1 cells. CRISPR-Cas9-edited hTERT-RPE1 cells with c.−69G>A variant in homozygous state showed loss of cilia or abnormal cilia (green) whereas the wild-type and heterozygous cells showed presence of cilia. The cilia were stained with acetylated tubulin (green) l and the nucleus were stained with DAPI (blue). The scale bar represents 10 μm. Two independent clones with each genotype were analyzed.
(G) Reduction in percent ciliated hTERT-RPE1 cells with c.−69G>A. Percent ciliated cells is significantly low when c.−69G>A variant is present in the homozygous (3%) or heterozygous (54%) state when compared to the wild-type. Corrected p value < 0.0001 (Kruskal-Wallis non-parametric test with Dunn's multiple comparison of the difference between all of the conditions).
(H) Total *TMEME216* expression in the human peripheral retina compared to all GTEx tissues. Distribution of total *TMEM216* expression in combined GTEx tissues (mean expression = 11.02 ± 0.05 TPM, n = 17,382) and the human peripheral retinal samples (mean expression = 19.96 ± 0.24 TPM, n = 411), showing a significantly higher expression in the retina (Mann Whitney nonparametric test p value < 0.0001).

with apparent normal gross morphology of cilia in cells with the heterozygous c.−69G>A genotype compared to the wild-type hTERT-RPE1 cells while a majority of cells homozygous for the c.−69G>A/c.−71C>T genotype lacked cilia (Figure 4F). The percentage of ciliated cells are significantly low among cells with the heterozygous and homozygous genotype compared to the wild-type (54% and 3% of wild-type, respectively, with adjusted *p* values of <0.0001) (Figure 4G). These findings suggested abnormal ciliogenesis in hTERT-RPE1 cells with c.−69G>A variant and reduced levels of *TMEM216* transcript. The impact of the additional variant c.−71C>T in cells with the homozygous genotype is unknown. Analysis of GTEx data revealed significantly higher levels of *TMEM216* transcript in the human peripheral retina compared to those recorded from additional tissues in the GTEx database (Figure 4H).[48,49]

Discussion

This study describes two non-coding variants in *TMEM216*, c.−69 G>A and c.−69G>T, as the likely underlying cause of non-syndromic RP in 74 affected individuals from 49 families of African and South Asian ancestry.

Forty-five individuals with recessive RP from 40 pedigrees have been found so far to be homozygous or compound heterozygous for the G>T change and 29 individuals from nine families have been found to be homozygous for the G>A variant. Two affected siblings were compound heterozygotes for the G>T variant and a deletion encompassing exons 1–3 of *TMEM216* and the upstream region. One affected individual was compound heterozygous for the G>T variant and a splice site variant c.35−2A>G. The c.35−2A>G substitution in *TMEM216* observed in one of the compound heterozygotes would only be expected to affect *TMEM216* specifically, consistent with the pathology being consequent on reduced *TMEM216* expression rather than an effect on other nearby genes.

The population frequencies reported for both variants are consistent with carrier frequencies in recessive IRD genes. Haplotype analysis is consistent with a single ancestral mutation event giving rise to all extant disease-associated alleles for each of the two variants. The relatively high prevalence of the G>T allele in the African population (0.005 in gnomAD) is noteworthy. This prevalence is higher, for instance, than the most common alleles causing recessive RP in the European population, e.g., *USH2A* (MIM: 608400; GenBank: NM_206933.4) (c.2299del [p.Glu767SerfsTer21] and c.2276G>T [p.Cys759Phe], with allele frequencies of 0.001 and 0.002, respectively).[45,50] Based on the allelic frequency, we can estimate 1 in 40,000 in this population would be homozygous for this variant. The sum of allelic frequencies of pathogenic and likely pathogenic variants from ClinVar as well as clear loss-of-function variants from gnomAD (v.4.0.0)[45] is 0.00033 for African/African American population (for nine variants). Therefore, we expect 1:300,000 individuals to carry the c.−69G>T variant in *trans* with a pathogenic variant. This makes the expected frequency of individuals carrying c.−69G>T homozygous or in *trans* with another pathogenic variant to ∼1:35,000 in that population. This would be expected to be a significant proportion of non-syndromic RP in this population.

The nature and location of the sequence encompassing the *TMEM216* c.−69G site and the *in silico* analysis suggest a critical role for this genomic region in transcriptional regulation of *TMEM216*. Four independent assays presented in our study (dual reporter Luciferase assay, RT-qPCR, and nanopore sequencing of affected individuals' leukocytes and RT-qPCR of edited cell lines) demonstrated that the c.−69 G>A or G>T noncoding variants downregulate *TMEM216* expression. Our experimental validations indicate that the *TMEM216* expression is reduced but not abrogated by these variants without affecting nearby IRD genes.

It is of interest that all individuals presented here (age range at exam 5–72 years) did not show any symptoms suggestive of the systemic pathology that occurs in affected individuals reported with bi-allelic variants in *TMEM216* which cause Joubert, Meckel, and related disorders.[24] None of the subjects with *TMEM216* c.−69G>A or G>T variants exhibited neurological symptoms. However, because neuroimaging was not clinically indicated, we cannot exclude asymptomatic minor structural changes in the cerebellum.

One possible explanation for the specificity of involvement of the rod photoreceptors in these individuals might be a need for higher *TMEM216* gene expression in these cells. This is supported by the presence of significantly higher levels of *TMEM216* transcript in the human peripheral retina compared to the levels listed in GTEx.[48,51] It is likely that the photoreceptor cells are more sensitive to the reduction of gene expression, and therefore the *TMEM216* c.−69G>A or G>T variants leading to such gene expression reduction, rather than complete loss of expression, cause specific dysfunction of photoreceptors. This phenomenon has been observed in other ciliopathy genes such as *CEP290* (MIM: 610142) which is associated with a spectrum of phenotypes ranging from Leber congenital amaurosis (LCA [MIM: 611755]), to the lethal Meckel syndrome (MKS).[18–23] However, cases have been reported with a lack of apparent retinal involvement in the individuals with homozygous c.218G>T (p.Arg73Leu) reported by Valente et al.[24] It is possible that the mechanism of disease of this mutation is different than the reduced expression/function caused by *TMEM216* c.−69G>A and G>T, which lead to differences in the retinal phenotype.

It is noted that there are at least two major transcripts generated from the human *TMEM216* gene. The longer transcript (GenBank: NM_001330285) has a shorter open reading frame (−87 amino acids compared with 148 from the shorter transcript [GenBank: NM_001173991.3]) due

to the use of a downstream start codon in the longer transcript. The presence of both isoforms is observed in the majority of tissues.[49] Our analysis of *TMEM216* transcripts in affected individuals' leukocytes to study the impact of *TMEM216* c.−69G>T in individuals with the c.−69G>T genotype in the homozygous and heterozygous states appeared to show similar reduction in both transcripts equally in the homo- and heterozygote on read-counting of nanopore-generated sequencing. It remains possible that one of the two transcripts is critical for rod photoreceptor function and maintenance and that the c.−69 variants have a specific effect on this specific retinal transcript. Additional studies are needed to understand the mechanism underlying non-syndromic RP phenotype due to the non-coding variants c.−69G>A and c.−69G>T. Notably, all *TMEM216* variants reported so far in individuals affected with Joubert syndrome involve only the coding sequence and would be expected to affect both isoforms.[24]

The TMEM216 protein is part of the "MKS module" that localizes to the cilia transition zone and plays a key role in ciliogenesis.[17,52,53] This complex includes additional proteins involved in ciliopathies.[54] The phenotypes observed in affected individuals with variants in *TMEM216* are Joubert and Meckel syndrome, which are severe ciliopathies that often involve retinal degeneration.[24,55,56] In previous studies, fibroblasts derived from individuals with *TMEM216* variants show impaired ciliogenesis.[24,25] It is well established that the integrity of cellular ciliary machinery is critical in the formation and maintenance of photoreceptors and as a result, variants in *TMEM216* are predicted to cause retinal degeneration along with other ciliary phenotypes.[53] Further, *Tmem216* knockdown zebrafish show abnormal outer segment formation compared to wild-type, while complete loss of *Tmem216* leads to embryonic and postnatal lethality in mice.[47,53] Consistent with the above observations, the hTERT-RPE1 cells with c.−69G>A genotype lacked cilia, indicating abnormal ciliogenesis.[24,47] These observations suggest the involvement of *TMEM216* in retinal pathology observed in individuals with the c.−69G>T and c.−69G>A variants upstream of this gene and abnormal ciliogenesis as a possible mechanism underlying retinal pathology.

Identification of noncoding variants with a high impact on gene expression that lead to IRD is an emerging phenomenon; for example, causative variants upstream of *PRDM13* (MIM: 616741) have been shown to cause North Carolina macular dystrophy (MCDR1 [MIM: 136550]).[57–59] We anticipate that such variants will be a major cause in the remaining genetically unsolved IRD cases. The identification of *TMEM216* c.−69 G>T and G>A described herein significantly improves the molecular diagnosis for IRD-affected individuals, particularly in those of African ethnicity who are historically understudied.[60–64] Despite their genetic diversity, there is a scarcity of available genetic data, which makes the interpretation of pathogenicity of variants more challenging.[45,65,66] Therefore, it is essential to perform rigorous validation studies to prove that such variants are pathogenic and to understand their mechanism of disease. These findings will open up the possibility of gene-directed therapies such as gene editing or augmentation.

Data and code availability

The metadata and the whole-exome/-genome sequencing data have been deposited in database of Genotypes and Phenotypes (dbGaP study IDs: phs001619.v2.p1, phs001272.v1.p1, and phs002459.v1.p1), UKBB, and 100KGenome. The data are available upon request.

Supplemental information

Supplemental information can be found online at https://doi.org/10.1016/j.ajhg.2024.07.020.

Declaration of interests

All the authors declare no competing interests.

Received: March 29, 2024
Accepted: July 29, 2024
Published: August 26, 2024

Web resources

Biorender, BioRender.com
Eukaryotic Promoter Database (EPD), https://epd.expasy.org
GenBank, https://www.ncbi.nlm.nih.gov/genbank/
minimap2 v.2.22, https://github.com/lh3/minimap2
OMIM, https://www.omim.org/
Porechop v.0.2.4, https://github.com/rrwick/Porechop
RetNet, http://www.sph.uth.tmc.edu/RetNet/
SAMtools v.1.9, http://www.htslib.org/

References

1. Carss, K.J., Arno, G., Erwood, M., Stephens, J., Sanchis-Juan, A., Hull, S., Megy, K., Grozeva, D., Dewhurst, E., Malka, S., et al. (2017). Comprehensive Rare Variant Analysis via Whole-Genome Sequencing to Determine the Molecular Pathology of Inherited Retinal Disease. Am. J. Hum. Genet. *100*, 75–90. https://doi.org/10.1016/j.ajhg.2016.12.003.
2. Hanany, M., Rivolta, C., and Sharon, D. (2020). Worldwide carrier frequency and genetic prevalence of autosomal recessive inherited retinal diseases. Proc. Natl. Acad. Sci. USA *117*, 2710–2716. https://doi.org/10.1073/pnas.1913179117.
3. Hartong, D.T., Berson, E.L., and Dryja, T.P. (2006). Retinitis pigmentosa. Lancet *368*, 1795–1809. https://doi.org/10.1016/s0140-6736(06)69740-7.
4. 100000 Genomes Project Pilot Investigators, Smedley, D., Smith, K.R., Martin, A., Thomas, E.A., McDonagh, E.M., Cipriani, V., Ellingford, J.M., Arno, G., Tucci, A., et al. (2021). 100,000 Genomes Pilot on Rare-Disease Diagnosis in Health Care - Preliminary Report. N. Engl. J. Med. *385*, 1868–1880. https://doi.org/10.1056/NEJMoa2035790.

5. Farrar, G.J., Carrigan, M., Dockery, A., Millington-Ward, S., Palfi, A., Chadderton, N., Humphries, M., Kiang, A.S., Kenna, P.F., and Humphries, P. (2017). Toward an elucidation of the molecular genetics of inherited retinal degenerations. Hum. Mol. Genet. *26*, R2–R11. https://doi.org/10.1093/hmg/ddx185.
6. Biswas, P., Villanueva, A.L., Soto-Hermida, A., Duncan, J.L., Matsui, H., Borooah, S., Kurmanov, B., Richard, G., Khan, S.Y., Branham, K., et al. (2021). Deciphering the genetic architecture and ethnographic distribution of IRD in three ethnic populations by whole genome sequence analysis. PLoS Genet. *17*, e1009848. https://doi.org/10.1371/journal.pgen.1009848.
7. Dueñas Rey, A., Del Pozo Valero, M., Bouckaert, M., Wood, K.A., Van den Broeck, F., Daich Varela, M., Thomas, H.B., Van Heetvelde, M., De Bruyne, M., Van de Sompele, S., et al. (2024). Combining a prioritization strategy and functional studies nominates 5'UTR variants underlying inherited retinal disease. Genome Med. *16*, 7. https://doi.org/10.1186/s13073-023-01277-1.
8. Quinodoz, M., Kaminska, K., Cancellieri, F., Han, J.H., Peter, V.G., Celik, E., Janeschitz-Kriegl, L., Schärer, N., Hauenstein, D., György, B., et al. (2024). Detection of elusive DNA copy-number variations in hereditary disease and cancer through the use of noncoding and off-target sequencing reads. Am. J. Hum. Genet. *111*, 701–713. https://doi.org/10.1016/j.ajhg.2024.03.001.
9. Sullivan, L.S., and Daiger, S.P. (1996). Inherited retinal degeneration: exceptional genetic and clinical heterogeneity. Mol. Med. Today *2*, 380–386. https://doi.org/10.1016/s1357-4310(96)10037-x.
10. Daich Varela, M., Bellingham, J., Motta, F., Jurkute, N., Ellingford, J.M., Quinodoz, M., Oprych, K., Niblock, M., Janeschitz-Kriegl, L., Kaminska, K., et al. (2023). Multidisciplinary team directed analysis of whole genome sequencing reveals pathogenic non-coding variants in molecularly undiagnosed inherited retinal dystrophies. Hum. Mol. Genet. *32*, 595–607. https://doi.org/10.1093/hmg/ddac227.
11. Bujakowska, K.M., Fernandez-Godino, R., Place, E., Consugar, M., Navarro-Gomez, D., White, J., Bedoukian, E.C., Zhu, X., Xie, H.M., Gai, X., et al. (2017). Copy-number variation is an important contributor to the genetic causality of inherited retinal degenerations. Genet. Med. *19*, 643–651. https://doi.org/10.1038/gim.2016.158.
12. Liu, Q., Tan, G., Levenkova, N., Li, T., Pugh, E.N., Jr., Rux, J.J., Speicher, D.W., and Pierce, E.A. (2007). The proteome of the mouse photoreceptor sensory cilium complex. Mol. Cell. Proteomics *6*, 1299–1317. https://doi.org/10.1074/mcp.M700054-MCP200.
13. den Hollander, A.I., Koenekoop, R.K., Mohamed, M.D., Arts, H.H., Boldt, K., Towns, K.V., Sedmak, T., Beer, M., Nagel-Wolfrum, K., McKibbin, M., et al. (2007). Mutations in LCA5, encoding the ciliary protein lebercilin, cause Leber congenital amaurosis. Nat. Genet. *39*, 889–895. https://doi.org/10.1038/ng2066.
14. Bujakowska, K.M., Zhang, Q., Siemiatkowska, A.M., Liu, Q., Place, E., Falk, M.J., Consugar, M., Lancelot, M.E., Antonio, A., Lonjou, C., et al. (2015). Mutations in IFT172 cause isolated retinal degeneration and Bardet-Biedl syndrome. Hum. Mol. Genet. *24*, 230–242. https://doi.org/10.1093/hmg/ddu441.
15. Chaki, M., Airik, R., Ghosh, A.K., Giles, R.H., Chen, R., Slaats, G.G., Wang, H., Hurd, T.W., Zhou, W., Cluckey, A., et al. (2012). Exome capture reveals ZNF423 and CEP164 mutations, linking renal ciliopathies to DNA damage response signaling. Cell *150*, 533–548. https://doi.org/10.1016/j.cell.2012.06.028.
16. Kim, S.K., Shindo, A., Park, T.J., Oh, E.C., Ghosh, S., Gray, R.S., Lewis, R.A., Johnson, C.A., Attie-Bittach, T., Katsanis, N., and Wallingford, J.B. (2010). Planar cell polarity acts through septins to control collective cell movement and ciliogenesis. Science *329*, 1337–1340. https://doi.org/10.1126/science.1191184.
17. Huang, L., Szymanska, K., Jensen, V.L., Janecke, A.R., Innes, A.M., Davis, E.E., Frosk, P., Li, C., Willer, J.R., Chodirker, B.N., et al. (2011). TMEM237 is mutated in individuals with a Joubert syndrome related disorder and expands the role of the TMEM family at the ciliary transition zone. Am. J. Hum. Genet. *89*, 713–730. https://doi.org/10.1016/j.ajhg.2011.11.005.
18. Coppieters, F., Lefever, S., Leroy, B.P., and De Baere, E. (2010). CEP290, a gene with many faces: mutation overview and presentation of CEP290base. Hum. Mutat. *31*, 1097–1108. https://doi.org/10.1002/humu.21337.
19. Leroy, B.P., Birch, D.G., Duncan, J.L., Lam, B.L., Koenekoop, R.K., Porto, F.B.O., Russell, S.R., and Girach, A. (2021). LEBER CONGENITAL AMAUROSIS DUE TO CEP290 MUTATIONS-SEVERE VISION IMPAIRMENT WITH A HIGH UNMET MEDICAL NEED: A Review. Retina *41*, 898–907. https://doi.org/10.1097/iae.0000000000003133.
20. Burnight, E.R., Wiley, L.A., Drack, A.V., Braun, T.A., Anfinson, K.R., Kaalberg, E.E., Halder, J.A., Affatigato, L.M., Mullins, R.F., Stone, E.M., and Tucker, B.A. (2014). CEP290 gene transfer rescues Leber congenital amaurosis cellular phenotype. Gene Ther. *21*, 662–672. https://doi.org/10.1038/gt.2014.39.
21. Perrault, I., Delphin, N., Hanein, S., Gerber, S., Dufier, J.L., Roche, O., Defoort-Dhellemmes, S., Dollfus, H., Fazzi, E., Munnich, A., et al. (2007). Spectrum of NPHP6/CEP290 mutations in Leber congenital amaurosis and delineation of the associated phenotype. Hum. Mutat. *28*, 416. https://doi.org/10.1002/humu.9485.
22. Frank, V., den Hollander, A.I., Brüchle, N.O., Zonneveld, M.N., Nürnberg, G., Becker, C., Du Bois, G., Kendziorra, H., Roosing, S., Senderek, J., et al. (2008). Mutations of the CEP290 gene encoding a centrosomal protein cause Meckel-Gruber syndrome. Hum. Mutat. *29*, 45–52. https://doi.org/10.1002/humu.20614.
23. Baala, L., Audollent, S., Martinovic, J., Ozilou, C., Babron, M.C., Sivanandamoorthy, S., Saunier, S., Salomon, R., Gonzales, M., Rattenberry, E., et al. (2007). Pleiotropic effects of CEP290 (NPHP6) mutations extend to Meckel syndrome. Am. J. Hum. Genet. *81*, 170–179. https://doi.org/10.1086/519494.
24. Valente, E.M., Logan, C.V., Mougou-Zerelli, S., Lee, J.H., Silhavy, J.L., Brancati, F., Iannicelli, M., Travaglini, L., Romani, S., Illi, B., et al. (2010). Mutations in TMEM216 perturb ciliogenesis and cause Joubert, Meckel and related syndromes. Nat. Genet. *42*, 619–625. https://doi.org/10.1038/ng.594.
25. Lee, J.H., Silhavy, J.L., Lee, J.E., Al-Gazali, L., Thomas, S., Davis, E.E., Bielas, S.L., Hill, K.J., Iannicelli, M., Brancati, F., et al. (2012). Evolutionarily assembled cis-regulatory module at a human ciliopathy locus. Science *335*, 966–969. https://doi.org/10.1126/science.1213506.
26. Perea-Romero, I., Blanco-Kelly, F., Sanchez-Navarro, I., Lorda-Sanchez, I., Tahsin-Swafiri, S., Avila-Fernandez, A., Martin-Merida, I., Trujillo-Tiebas, M.J., Lopez-Rodriguez, R., Rodriguez de Alba, M., et al. (2021). NGS and phenotypic ontology-based approaches increase the diagnostic yield in

syndromic retinal diseases. Hum. Genet. *140*, 1665–1678. https://doi.org/10.1007/s00439-021-02343-7.
27. Hartill, V., Szymanska, K., Sharif, S.M., Wheway, G., and Johnson, C.A. (2017). Meckel-Gruber Syndrome: An Update on Diagnosis, Clinical Management, and Research Advances. Front. Pediatr. *5*, 244. https://doi.org/10.3389/fped.2017.00244.
28. Bergmann, C., Frank, V., and Salonen, R. (2016). Clinical utility gene card for: Meckel syndrome - update 2016. Eur. J. Hum. Genet. *24*. https://doi.org/10.1038/ejhg.2016.33.
29. Szymanska, K., Berry, I., Logan, C.V., Cousins, S.R., Lindsay, H., Jafri, H., Raashid, Y., Malik-Sharif, S., Castle, B., Ahmed, M., et al. (2012). Founder mutations and genotype-phenotype correlations in Meckel-Gruber syndrome and associated ciliopathies. Cilia *1*, 18. https://doi.org/10.1186/2046-2530-1-18.
30. Biswas, P., Duncan, J.L., Ali, M., Matsui, H., Naeem, M.A., Raghavendra, P.B., Frazer, K.A., Arts, H.H., Riazuddin, S., Akram, J., et al. (2017). A mutation in IFT43 causes non-syndromic recessive retinal degeneration. Hum. Mol. Genet. *26*, 4741–4751. https://doi.org/10.1093/hmg/ddx356.
31. McKenna, A., Hanna, M., Banks, E., Sivachenko, A., Cibulskis, K., Kernytsky, A., Garimella, K., Altshuler, D., Gabriel, S., Daly, M., and DePristo, M.A. (2010). The Genome Analysis Toolkit: a MapReduce framework for analyzing next-generation DNA sequencing data. Genome Res. *20*, 1297–1303. https://doi.org/10.1101/gr.107524.110.
32. Quinodoz, M., Peter, V.G., Bedoni, N., Royer Bertrand, B., Cisarova, K., Salmaninejad, A., Sepahi, N., Rodrigues, R., Piran, M., Mojarrad, M., et al. (2021). AutoMap is a high performance homozygosity mapping tool using next-generation sequencing data. Nat. Commun. *12*, 518. https://doi.org/10.1038/s41467-020-20584-4.
33. McCulloch, D.L., Marmor, M.F., Brigell, M.G., Hamilton, R., Holder, G.E., Tzekov, R., and Bach, M. (2015). ISCEV Standard for full-field clinical electroretinography (2015 update). Doc. Ophthalmol. *130*, 1–12. https://doi.org/10.1007/s10633-014-9473-7.
34. Grant, C.E., Bailey, T.L., and Noble, W.S. (2011). FIMO: scanning for occurrences of a given motif. Bioinformatics *27*, 1017–1018. https://doi.org/10.1093/bioinformatics/btr064.
35. Kulakovskiy, I.V., Vorontsov, I.E., Yevshin, I.S., Sharipov, R.N., Fedorova, A.D., Rumynskiy, E.I., Medvedeva, Y.A., Magana-Mora, A., Bajic, V.B., Papatsenko, D.A., et al. (2018). HOCOMOCO: towards a complete collection of transcription factor binding models for human and mouse via large-scale ChIP-Seq analysis. Nucleic Acids Res. *46*, D252–D259. https://doi.org/10.1093/nar/gkx1106.
36. Sandelin, A., Alkema, W., Engström, P., Wasserman, W.W., and Lenhard, B. (2004). JASPAR: an open-access database for eukaryotic transcription factor binding profiles. Nucleic Acids Res. *32*, D91–D94. https://doi.org/10.1093/nar/gkh012.
37. Thomas, E.D., Timms, A.E., Giles, S., Harkins-Perry, S., Lyu, P., Hoang, T., Qian, J., Jackson, V.E., Bahlo, M., Blackshaw, S., et al. (2022). Cell-specific cis-regulatory elements and mechanisms of non-coding genetic disease in human retina and retinal organoids. Dev. Cell *57*, 820–836.e6. https://doi.org/10.1016/j.devcel.2022.02.018.
38. Rao, X., Huang, X., Zhou, Z., and Lin, X. (2013). An improvement of the 2(-delta delta CT) method for quantitative real-time polymerase chain reaction data analysis. Biostat. Bioinforma. Biomath. *3*, 71–85.
39. Wick, R.R., Judd, L.M., Gorrie, C.L., and Holt, K.E. (2017). Completing bacterial genome assemblies with multiplex MinION sequencing. Microb. Genom. *3*, e000132. https://doi.org/10.1099/mgen.0.000132.
40. De Coster, W., D'Hert, S., Schultz, D.T., Cruts, M., and Van Broeckhoven, C. (2018). NanoPack: visualizing and processing long-read sequencing data. Bioinformatics *34*, 2666–2669. https://doi.org/10.1093/bioinformatics/bty149.
41. Li, H. (2018). Minimap2: pairwise alignment for nucleotide sequences. Bioinformatics *34*, 3094–3100. https://doi.org/10.1093/bioinformatics/bty191.
42. Danecek, P., Bonfield, J.K., Liddle, J., Marshall, J., Ohan, V., Pollard, M.O., Whitwham, A., Keane, T., McCarthy, S.A., Davies, R.M., and Li, H. (2021). Twelve years of SAMtools and BCFtools. GigaScience *10*, giab008. https://doi.org/10.1093/gigascience/giab008.
43. Robinson, J.T., Thorvaldsdóttir, H., Winckler, W., Guttman, M., Lander, E.S., Getz, G., and Mesirov, J.P. (2011). Integrative genomics viewer. Nat. Biotechnol. *29*, 24–26. https://doi.org/10.1038/nbt.1754.
44. Mandal, M.N.A., Vasireddy, V., Jablonski, M.M., Wang, X., Heckenlively, J.R., Hughes, B.A., Reddy, G.B., and Ayyagari, R. (2006). Spatial and temporal expression of MFRP and its interaction with CTRP5. Invest. Ophthalmol. Vis. Sci. *47*, 5514–5521. https://doi.org/10.1167/iovs.06-0449.
45. Karczewski, K.J., Francioli, L.C., Tiao, G., Cummings, B.B., Alföldi, J., Wang, Q., Collins, R.L., Laricchia, K.M., Ganna, A., Birnbaum, D.P., et al. (2020). The mutational constraint spectrum quantified from variation in 141,456 humans. Nature *581*, 434–443. https://doi.org/10.1038/s41586-020-2308-7.
46. Dreos, R., Ambrosini, G., Groux, R., Cavin Périer, R., and Bucher, P. (2017). The eukaryotic promoter database in its 30th year: focus on non-vertebrate organisms. Nucleic Acids Res. *45*, D51–D55. https://doi.org/10.1093/nar/gkw1069.
47. Wang, Y., Yao, H., Zhang, Y., Mu, N., Lu, T., Du, Z., Wu, Y., Li, X., Su, M., Shao, M., et al. (2024). TMEM216 promotes primary ciliogenesis and Hedgehog signaling through the SUFU-GLI2/GLI3 axis. Sci. Signal. *17*, eabo0465. https://doi.org/10.1126/scisignal.abo0465.
48. GTEx Consortium (2020). The GTEx Consortium atlas of genetic regulatory effects across human tissues. Science *369*, 1318–1330. https://doi.org/10.1126/science.aaz1776.
49. GTEx Consortium (2013). The Genotype-Tissue Expression (GTEx) project. Nat. Genet. *45*, 580–585. https://doi.org/10.1038/ng.2653.
50. Lin, S., Vermeirsch, S., Pontikos, N., Martin-Gutierrez, M.P., Daich Varela, M., Malka, S., Schiff, E., Knight, H., Wright, G., Jurkute, N., et al. (2024). Spectrum of Genetic Variants in the Most Common Genes Causing Inherited Retinal Disease in a Large Molecularly Characterized United Kingdom Cohort. Ophthalmol. Retina *8*, 699–709. https://doi.org/10.1016/j.oret.2024.01.012.
51. Ratnapriya, R., Sosina, O.A., Starostik, M.R., Kwicklis, M., Kapphahn, R.J., Fritsche, L.G., Walton, A., Arvanitis, M., Gieser, L., Pietraszkiewicz, A., et al. (2019). Retinal transcriptome and eQTL analyses identify genes associated with age-related macular degeneration. Nat. Genet. *51*, 606–610. https://doi.org/10.1038/s41588-019-0351-9.
52. Garcia-Gonzalo, F.R., Corbit, K.C., Sirerol-Piquer, M.S., Ramaswami, G., Otto, E.A., Noriega, T.R., Seol, A.D., Robinson, J.F., Bennett, C.L., Josifova, D.J., et al. (2011). A Transition Zone Complex Regulates Mammalian Ciliogenesis and Ciliary

Membrane Composition. Nat. Genet *43*, 776–784. https://doi.org/10.1038/ng.891.

53. Liu, Y., Cao, S., Yu, M., and Hu, H. (2020). TMEM216 Deletion Causes Mislocalization of Cone Opsin and Rhodopsin and Photoreceptor Degeneration in Zebrafish. Invest. Ophthalmol. Vis. Sci. *61*, 24. https://doi.org/10.1167/iovs.61.8.24.
54. Van De Weghe, J.C., Gomez, A., and Doherty, D. (2022). The Joubert-Meckel-Nephronophthisis Spectrum of Ciliopathies. Annu. Rev. Genom. Hum. Genet. *23*, 301–329. https://doi.org/10.1146/annurev-genom-121321-093528.
55. Edvardson, S., Shaag, A., Zenvirt, S., Erlich, Y., Hannon, G.J., Shanske, A.L., Gomori, J.M., Ekstein, J., and Elpeleg, O. (2010). Joubert syndrome 2 (JBTS2) in Ashkenazi Jews is associated with a TMEM216 mutation. Am. J. Hum. Genet. *86*, 93–97. https://doi.org/10.1016/j.ajhg.2009.12.007.
56. Serpieri, V., Mortarini, G., Loucks, H., Biagini, T., Micalizzi, A., Palmieri, I., Dempsey, J.C., D'Abrusco, F., Mazzotta, C., Battini, R., et al. (2023). Recurrent, founder and hypomorphic variants contribute to the genetic landscape of Joubert syndrome. J. Med. Genet. *60*, 885–893. https://doi.org/10.1136/jmg-2022-108725.
57. Small, K.W., DeLuca, A.P., Whitmore, S.S., Rosenberg, T., Silva-Garcia, R., Udar, N., Puech, B., Garcia, C.A., Rice, T.A., Fishman, G.A., et al. (2016). North Carolina Macular Dystrophy Is Caused by Dysregulation of the Retinal Transcription Factor PRDM13. Ophthalmology *123*, 9–18. https://doi.org/10.1016/j.ophtha.2015.10.006.
58. Silva, R.S., Arno, G., Cipriani, V., Pontikos, N., Defoort-Dhellemmes, S., Kalhoro, A., Carss, K.J., Raymond, F.L., Dhaenens, C.M., Jensen, H., et al. (2019). Unique noncoding variants upstream of PRDM13 are associated with a spectrum of developmental retinal dystrophies including progressive bifocal chorioretinal atrophy. Hum. Mutat. *40*, 578–587. https://doi.org/10.1002/humu.23715.
59. Van de Sompele, S., Small, K.W., Cicekdal, M.B., Soriano, V.L., D'Haene, E., Shaya, F.S., Agemy, S., Van der Snickt, T., Rey, A.D., Rosseel, T., et al. (2022). Multi-omics approach dissects cis-regulatory mechanisms underlying North Carolina macular dystrophy, a retinal enhanceropathy. Am. J. Hum. Genet. *109*, 2029–2048. https://doi.org/10.1016/j.ajhg.2022.09.013.
60. Onyango, O., Mureithi, M., Kithinji, D., Jaoko, W., and Fujinami, K. (2023). Challenges and Opportunities in the Genetic Analysis of Inherited Retinal Dystrophies in Africa, a Literature Review. J. Personalized Med. *13*, 239. https://doi.org/10.3390/jpm13020239.
61. Maltese, P.E., Colombo, L., Martella, S., Rossetti, L., El Shamieh, S., Sinibaldi, L., Passarelli, C., Coppè, A.M., Buzzonetti, L., Falsini, B., et al. (2022). Genetics of Inherited Retinal Diseases in Understudied Ethnic Groups in Italian Hospitals. Front. Genet. *13*, 914345. https://doi.org/10.3389/fgene.2022.914345.
62. Bouzidi, A., Charif, M., Bouzidi, A., Amalou, G., Kandil, M., Barakat, A., and Lenaers, G. (2021). Clinical and genetic investigations of three Moroccan families with retinitis pigmentosa phenotypes. Mol. Vis. *27*, 17–25.
63. Bouzidi, A., Charoute, H., Charif, M., Amalou, G., Kandil, M., Barakat, A., and Lenaers, G. (2022). Clinical and genetic spectrums of 413 North African families with inherited retinal dystrophies and optic neuropathies. Orphanet J. Rare Dis. *17*, 197. https://doi.org/10.1186/s13023-022-02340-7.
64. Roberts, L., Rebello, G., Greenberg, J., and Ramesar, R. (2019). Update on Inherited Retinal Disease in South Africa: Encouraging Diversity in Molecular Genetics. Adv. Exp. Med. Biol. *1185*, 257–261. https://doi.org/10.1007/978-3-030-27378-1_42.
65. Choudhury, A., Aron, S., Botigué, L.R., Sengupta, D., Botha, G., Bensellak, T., Wells, G., Kumuthini, J., Shriner, D., Fakim, Y.J., et al. (2020). High-depth African genomes inform human migration and health. Nature *586*, 741–748. https://doi.org/10.1038/s41586-020-2859-7.
66. Omotoso, O.E., Teibo, J.O., Atiba, F.A., Oladimeji, T., Adebesin, A.O., and Babalghith, A.O. (2022). Bridging the genomic data gap in Africa: implications for global disease burdens. Glob. Health *18*, 103. https://doi.org/10.1186/s12992-022-00898-2.